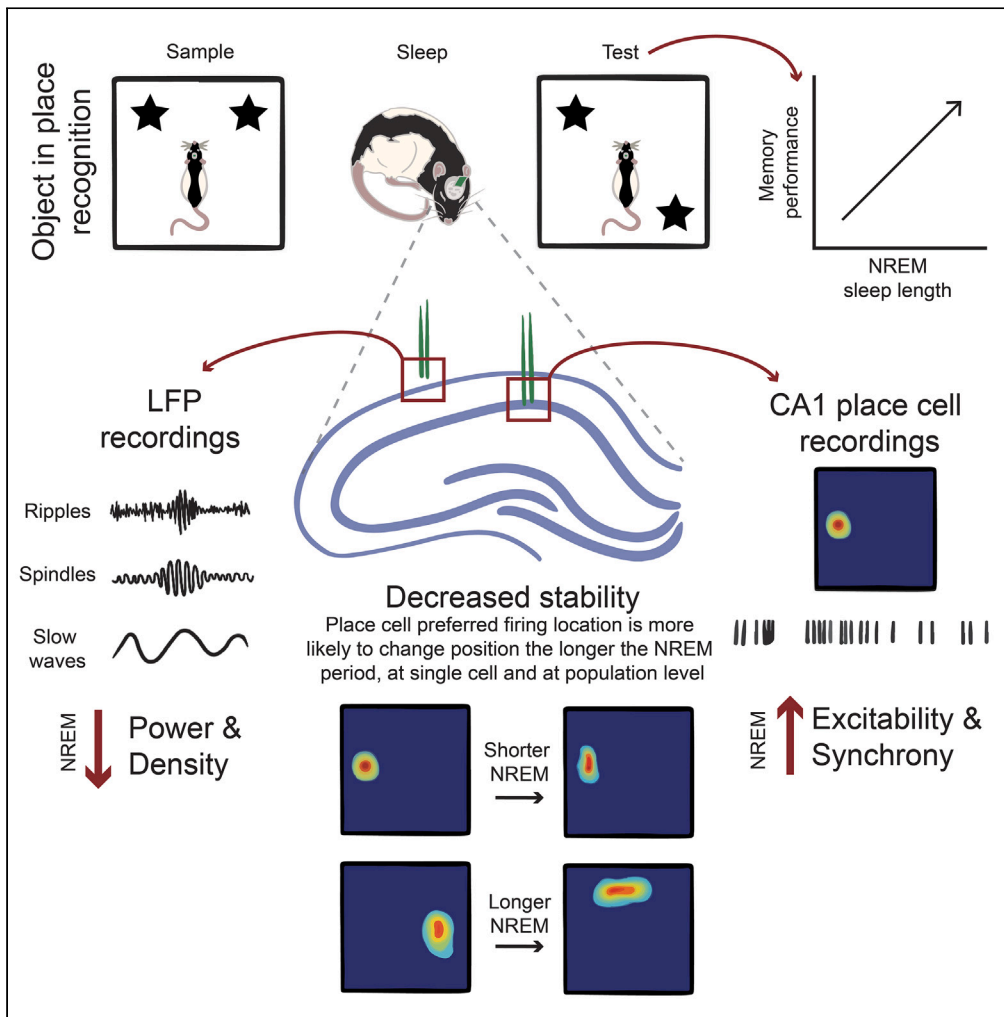


Article

Sleep-dependent decorrelation of hippocampal spatial representations



Gonzalo Valdivia, Nelson Espinosa, Ariel Lara-Vasquez, Mauricio Caneo, Marion Inostroza, Jan Born, Pablo Fuentealba

pjfuentealba@gmail.com

Highlights

Spatial memory retrieval linearly correlates with non-REM sleep duration

Cortical oscillations and hippocampal unit spiking decrease during non-REM sleep

Place cells synchronize more with sleep oscillations than non-encoding cells

Stability of hippocampal spatial representations decreases during non-REM sleep

Valdivia et al., iScience 27, 110076
June 21, 2024 © 2024 The Author(s). Published by Elsevier Inc.
<https://doi.org/10.1016/j.isci.2024.110076>



Article

Sleep-dependent decorrelation
of hippocampal spatial representations

Gonzalo Valdivia,^{1,3} Nelson Espinosa,^{1,3} Ariel Lara-Vasquez,¹ Mauricio Caneo,¹ Marion Inostroza,² Jan Born,²
and Pablo Fuentealba^{1,4,*}

SUMMARY

Neuronal ensembles are crucial for episodic memory and spatial mapping. Sleep, particularly non-REM (NREM), is vital for memory consolidation, as it triggers plasticity mechanisms through brain oscillations that reactivate neuronal ensembles. Here, we assessed their role in consolidating hippocampal spatial representations during sleep. We recorded hippocampus activity in rats performing a spatial object-place recognition (OPR) memory task, during encoding and retrieval periods, separated by intervening sleep. Successful OPR retrieval correlated with NREM duration, during which cortical oscillations decreased in power and density as well as neuronal spiking, suggesting global downregulation of network excitability. However, neurons encoding specific spatial locations (i.e., place cells) or objects during OPR showed stronger synchrony with brain oscillations compared to non-encoding neurons, and the stability of spatial representations decreased proportionally with NREM duration. Our findings suggest that NREM sleep may promote flexible remapping in hippocampal ensembles, potentially aiding memory consolidation and adaptation to novel spatial contexts.

INTRODUCTION

Sleep has been established as fundamental for episodic memory consolidation.^{1–4} Indeed, sleep deprivation after training episodic and spatial tasks impairs memory formation, whereas memory performance improves when sleep follows task training.^{5–7} Significantly, non-REM sleep (NREM) seems to be critical for the consolidation of episodic memory traces, as shown both in animals^{8–10} and humans.^{11–13} Repeated neuronal reactivations during NREM transform episodic representations from previous wake experience into long-term memories.¹⁴ Such a role is also supported by distinct sleep oscillations, i.e., hippocampal sharp-wave ripples (100–250 Hz),¹⁵ thalamic spindles (8–16 Hz),¹⁶ and cortical slow wave activity (0.5–4 Hz),¹⁷ which emerge and synchronize during NREM^{14,18–20} recruiting diverse brain regions and resulting in temporal windows of enhanced synaptic plasticity, which enable Hebbian mechanisms by temporally coalescing neuronal firing.^{8,21,22} Importantly, cortical recordings during spontaneous sleep-wake cycles in rats have shown that neuronal dynamics change as a function of sleep homeostasis.^{23,24} That is, neuronal firing rates and neuronal synchrony progressively decrease as sleep episodes evolve over time.²⁴ Being a time-evolving, dynamic brain state, sleep is associated with a decrease in power of oscillatory events, such as slow wave activity, including the slow oscillation, as well as in cortical excitability and neuronal firing rates.^{25,26} Conversely, hippocampal neurons have been found to increase their synchrony across sleep, specifically when synchronized to ripples, whereas overall firing rates also decrease in hippocampal networks.²⁷ To what extent the hippocampus participates in global downregulation during sleep is currently not clear.²⁸

Hippocampal place cells, signaling specific locations when animals navigate the environment,²⁹ are considered to encode a cognitive map in which episodic events are embedded.^{30,31} However, this cognitive map is not a fixed, permanent construct as it is strongly determined by experience. An example is the case of context-dependent remapping³² which refers to the relocation of place fields upon changes in the spatial environment.^{33–36} Unexpectedly, little information is currently available about the influence of sleep dynamics on the hippocampal spatial map. That is, whether and in which direction the sleep process affects hippocampal spatial representations. Here, we tested the hypothesis that sleep regulates activity of hippocampal networks such that spatial representations are preserved. Our results, indeed, show that NREM is key to the consolidation process during sleep in that the longer time an animal spends in NREM after spatial encoding, the better the memory is retrieved later on. Simultaneously, however, NREM duration is linked to a stronger decorrelation of spiking activity in the ensembles contributing to the representation, when (at OPR retrieval testing) the animal is exposed to a change in the spatial configuration of objects, suggesting that NREM enhances the capability of the hippocampal network for flexibly remapping and newly encode spatial features.

¹Laboratory of Neural Circuits, Departamento de Psiquiatría, Facultad de Medicina, Pontificia Universidad Católica de Chile. Santiago, Chile

²Institute of Medical Psychology and Behavioral Neurobiology, University of Tübingen, Tübingen, Germany

³These authors contributed equally

⁴Lead contact

*Correspondence: pjfuentealba@gmail.com

<https://doi.org/10.1016/j.isci.2024.110076>



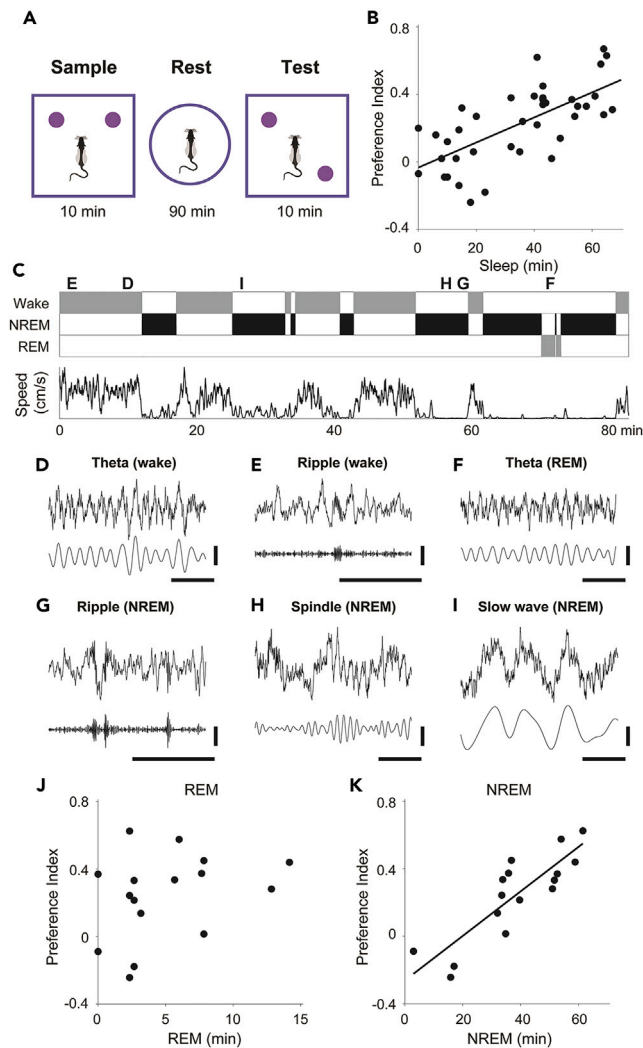


Figure 1. Sleep duration correlates with spatial memory consolidation

(A) Schematic of the object-in-place recognition (OPR) task.

(B) Preference index for the displaced object, indicative of spatial memory formation, positively correlates with sleep duration during the rest phase of the task ($p = 5.7 \times 10^{-7}$, $r = 0.70$, Pearson's linear correlation; $n = 40$ sessions; 22 sessions from 8 non-implanted rats were scored visually, 16 sessions from 4 implanted animals were scored visually and electrophysiologically).

(C) Example hypnogram and body speed from one rest session from an implanted animal (rat GV15, session 08).

(D–I) Example brain oscillations recorded in the dorsal CA1 during different brain states. Unfiltered LFP (top traces) and filtered oscillations (bottom traces). Theta (LFP filtered 4–8 Hz), ripples (LFP filtered 100–250 Hz), spindles (LFP filtered 8–15 Hz), slow wave activity (0.5–4 Hz).

(J and K) Spatial memory performance in relation to REM sleep duration (J, $p = 0.26$, $r = 0.30$, Pearson's linear correlation, $n = 16$ sessions, 4 implanted rats) or NREM duration (K, $p = 2.9 \times 10^{-5}$, $r = 0.85$, Pearson's linear correlation, $n = 16$ sessions, 4 implanted rats). Only significant regressions are plotted. See also Figures S1–S3 and S11.

RESULTS

Non-REM sleep duration correlates with increased spatial memory performance and decreased power of sleep oscillations

We trained a group of adult rats in the object-place recognition (OPR) task, a well-established spatial memory test,^{37,38} and allowed animals to freely sleep during a fixed resting period (90 min, Figure 1A). In initial experiments, sleep was visually identified by prolonged periods of immobility and the characteristic curled body posture³⁹ (Figure S1). Consistent with previous work^{37,40} we found a relation such that the cumulative duration of spontaneous sleep periods strongly predicted spatial discrimination during the retrieval phase, as longer sleep intervals were positively correlated with larger preference indexes, indicative of better spatial memory recall (Figures 1B and S2).

Next, we used hippocampal field potentials in combination with video monitoring of body movements to dissect sleep phases,⁴¹ and hypnograms were constructed for every resting session, differentiating two sleep stages (Figures 1C and S3). During wakefulness, theta oscillations

were prominent in the hippocampus during animal movement (Figure 1D) and ripples (100–250 Hz) emerged during quiescence (Figure 1E). In contrast, rapid eye movement (REM) sleep was defined by sustained theta oscillations during prolonged immobility periods (Figure 1F); whereas NREM was dominated by ripple episodes (Figure 1G), in combination with spindle oscillations (10–16 Hz, Figure 1H) or slow wave activity (0.5–4 Hz, Figure 1I). When sorting out by sleep phase, we found that REM sleep was not associated with spatial memory performance (Figure 1J), whereas the time spent in NREM was strongly correlated with spatial memory (Figure 1K). Indeed, a mediation analysis including both sleep stages (REM and NREM) showed that only NREM was significantly associated with memory performance ($p = 2.27 \times 10e-4$).^{37,42} NREM duration was a most powerful predictor of memory performance as it accounted for 80% of the total variance in spatial memory performance as indicated by the discrimination index. This result corroborates previous observations in both humans⁴³ and animals.^{37,42,44}

Sleep cardinal oscillations (slow waves, spindles, and ripples) are believed to be essential for memory consolidation.^{9,18,38} Hence, we focused on the dynamics of cortical oscillations across sleep (Figure 2). We found that hippocampal ripples, thalamocortical spindles, and cortical slow wave activity decreased in amplitude during NREM. Indeed, comparing the amplitude between oscillatory events during early (first 5 min) and late sleep (last 5 min), revealed a significant decrease in all three types of oscillation ($p < 0.05$, Figures 2A–2F). Also, the density (i.e., events per minute) of ripples and spindles decreased with time in NREM ($p < 0.001$, Figures 2G and 2H), while the power of slow wave activity decreased with increasing time in NREM ($p = 0.01$, Figure 2I). For slow wave activity, we noticed distinct peaks corresponding to slow oscillations (~1 Hz) and delta waves (2–4 Hz), which have been hypothesized to perform different roles in memory processing.⁴⁵ Hence, we subdivided the slow wave activity in these two bands and found that the same negative trend was present in both oscillatory patterns (Figure S4). The decrease in slow wave activity was apparent even in individual sleep bouts (Figure S5). Overall, the dynamics of sleep oscillations were found to be correlated with the temporal evolution of NREM, showing decreased amplitude, density, and power, consistent with previous work analyzing more extended periods of sleep [e.g., ref. ²⁴].

Preserved excitability and synchrony of place cells across non-REM sleep

Focusing on the neuronal firing dynamics during NREM, we found that the overall firing rate progressively decreased across NREM epochs with these dynamics differing between (regular firing, putative) pyramidal cells and (fast spiking, putative) interneurons. Pyramidal cells significantly reduced firing rates across sleep (Figures 3A and 3B), whereas the activity of interneurons remained relatively stable (Figures 3C and 3D). We then assessed neuronal synchrony by analyzing the coordinated spike timing of hippocampal neurons as determined by the average pairwise correlation coefficient.⁴⁶ Divergent from foregoing reports showing that neuronal synchrony of hippocampal principal cells increases across sleep²⁷ we found that overall synchronous spiking activity followed the same pattern as firing rates. That is, the average synchrony between pyramidal cells decreased across NREM (Figures 3E and 3F), whereas interneuron synchrony remained unaffected (Figures 3G and 3H). Thus, both firing rates and neuronal synchrony exhibited consistent patterns across NREM, which were distinct for pyramidal cells and interneurons. We further divided pyramidal cells according to their spatial information content. Indeed, we identified place cells by establishing their place fields during spatial exploration of the task arena, as well as ‘non-spatial cells’, detected by their negligible spatial information content (see STAR methods). As previously described, interneurons were the most active cell type, followed in sequence by place cells, and then non-spatial cells (Figure S6). During NREM, we observed a reduction in the average firing rate and synchrony of non-spatial cells. In contrast, place cells demonstrated a distinct pattern, maintaining their excitability and synchrony consistently throughout the NREM period. (Figure S7). This result suggests that while non-spatial cells were progressively down-regulated during sleep, the activity and synchrony of place cells were preserved.

Based on reports of a tight coupling between cortical slow waves, thalamocortical spindles, and hippocampal ripples with hippocampal neuronal firing during sleep,^{45,46} we next investigated the synchronization between sleep oscillations and individual hippocampal neurons.^{25,38,43} For this purpose, we computed event-correlation histograms of spike firing in dorsal CA1 time-locked to the peak of ripple events, the onset of spindle events, and the upstate of slow wave activity (Figures 4A–4C). This analysis, indeed, confirmed that each of these types of event was associated with an increase in neuronal discharge. On average, non-spatial cells showed lower recruitment compared to other cell types across sleep oscillations. Conversely, place cells showed the highest activation during sharp wave ripples, whereas interneurons exhibited the strongest coupling to spindles and slow waves (Figures 4D–4F). This pattern of correlations suggests that firing of place cells remained responsive to the brain oscillatory entrainment, although slow wave activity showed an overall decrease in amplitude across sleep. It has been shown that neuronal spiking varies with brain state.^{47–50} Accordingly, we observed that firing rates of putative pyramidal cells spanned a wide range of several orders of magnitude (Figure S8). There was a strong correlation between firing rates during NREM sleep and waking states ($R = 0.58$, $p = 8.3 \times 10e-28$). Consistent with earlier findings, the slope of this relationship deviated from the identity line,⁴⁹ suggesting that transitions in brain state differentially influence neurons depending on their activity levels (Figure S8). Specifically, neurons with lower firing rates during wakefulness showed increased activity during sleep, whereas those with higher rates during wakefulness showed decreased activity during sleep (Figure S8). To further investigate how sleep oscillations modulate spike timing, we divided putative pyramidal cells into five 20-percentile quintiles based on their firing rates. We then reanalyzed the synchrony between the firing of individual neurons and sleep oscillations for each quintile (Figure S8). Our results show that sleep oscillations differentially affect neurons based on their firing rates, with low-firing rate neurons showing weak coupling to sleep oscillations, which progressively increased in high-firing rate neurons (Figure S8).

Task-engaged cells robustly reactivate during non-REM sleep

According to the assumption that sleep consolidates memory, neurons recruited during waking experience are selectively reactivated during NREM, particularly within hippocampal ripples.^{51,52} Given the relevance of the spatial object configuration for memory formation in the OPR

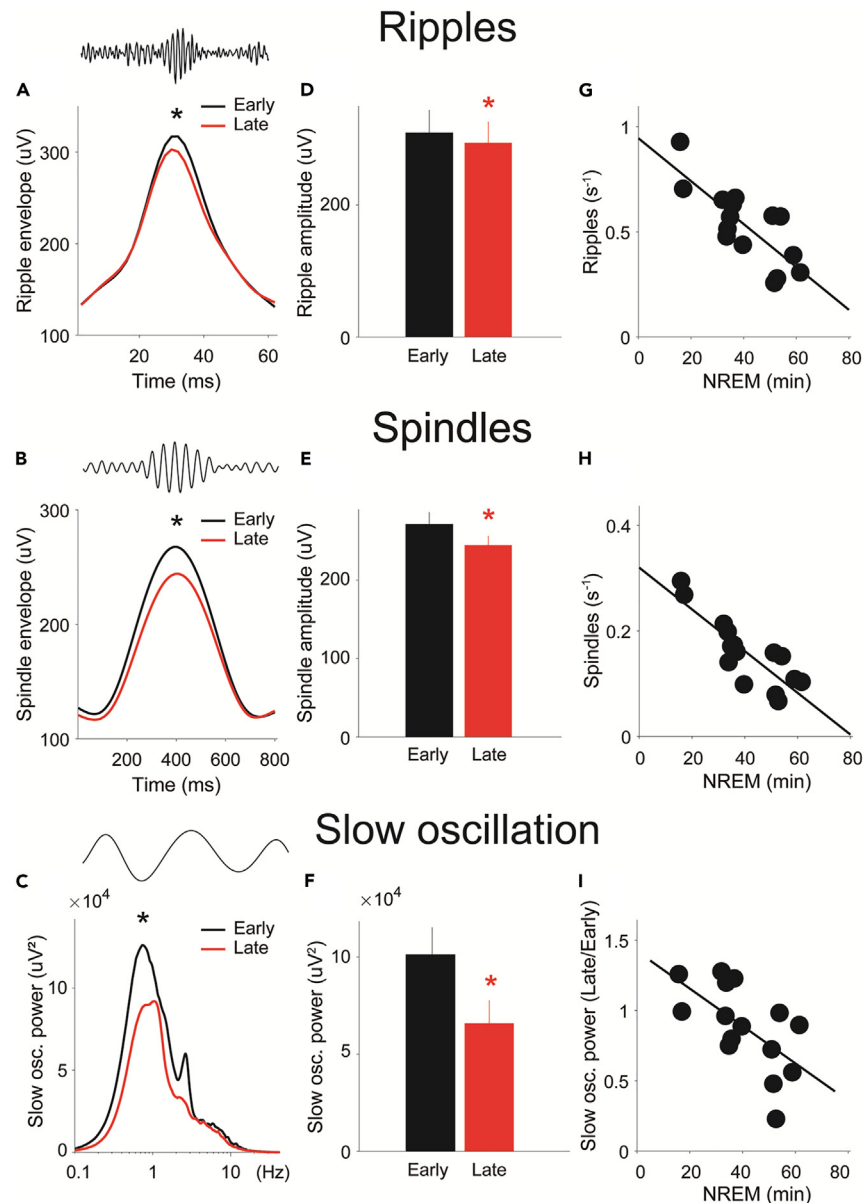


Figure 2. The power of brain oscillations decreases across sleep

(A–C) Average amplitude of cortical oscillations recorded in the dorsal CA1 calculated during early (black, first 5 min) and late (red, last 5 min) periods of NREM for ripples (A), spindles (B), and slow wave activity (C). Note distinct power peaks for slow oscillations (0.8 Hz) and delta waves (2.5 Hz) for slow wave activity (C). Top traces depict individual examples from filtered LFP traces.

(D–F) Amplitude comparison between early and late periods of NREM for ripples (D, $p = 0.012$, one sample paired t-test), spindles (E, $p = 5.7 \times 10^{-3}$, one sample paired t-test), and slow wave activity (F, $p = 0.007$, Wilcoxon signed rank test).

(G–I) Density of cortical oscillations during sleep in relation to NREM duration for ripples (G, $r = 0.79$, $p = 4.5 \times 10^{-4}$, Pearson's linear correlation) and spindles (H, $r = 0.85$, $p = 6.9 \times 10^{-5}$, Pearson's linear correlation), and power of slow wave activity in relation to NREM duration (I, $r = -0.64$, $p = 0.01$, Pearson's linear correlation). ($n = 16$ sessions, 4 rats). See also [Figures S4](#) and [S5](#).

task, we assessed hippocampal neuronal activity during object exploration. To this end, we first identified neurons that were selectively activated during object exploration. We found a sizable subpopulation of hippocampal units ($n = 114$, 45.6%, here termed 'object cells'), increasing discharge during object exploration (Figure 5A). Nearly half of the object cells were place cells ($n = 47$, 41.2%), as they showed a place field in the arena. Most object cells signaled either the immobile object ($n = 69$, 60.5%) or the displaced object ($n = 37$, 32.5%) during both the sample and test sessions, with only a few units discharging to both objects ($n = 8$, 7%). Moreover, pairwise peak cross-correlations of hippocampal unit activity during sleep were significantly larger for object cells than for non-encoding neurons, specifically during NREM

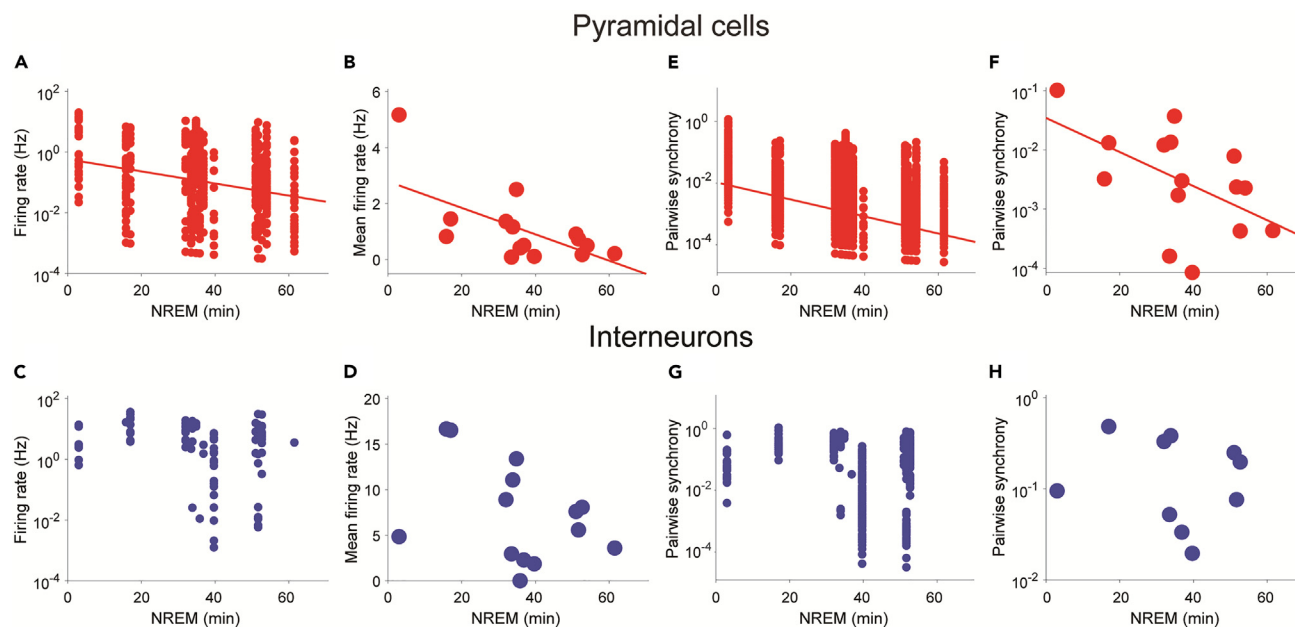


Figure 3. Firing rate and synchrony of hippocampal principal neurons decline across sleep

(A and C) Mean firing rate of pyramidal cells (A, $r = -0.19$, $p = 2.6 \times 10^{-5}$, Pearson's linear correlation) and interneurons (C, $r = -0.17$, $p = 0.08$, Pearson's linear correlation) in relation to NREM cumulative duration. Each dot represents a single recorded unit (pyramidal cells, $n = 515$; interneurons, $n = 97$).

(B and D) Mean firing rate of pyramidal cells (B, $r = 0.38$, $p = 0.01$, Pearson's linear correlation) and interneurons (D, $r = 0.09$, $p = 0.29$, Pearson's linear correlation) in relation to NREM cumulative duration. Each dot represents the average firing rate from all single units recorded per session.

(E and G) Pairwise synchrony of pyramidal cells (E, $r = -0.28$, $p = 2.1 \times 10^{-194}$, Pearson's linear correlation) and interneurons (G, $r = -0.2$, $p = 3.9 \times 10^{-9}$, Pearson's linear correlation) in relation to NREM cumulative duration. Each dot represents a pair of single units. F and H, mean pairwise synchrony of pyramidal cells (F, $r = -0.63$, $p = 0.01$, Pearson's linear correlation) and interneurons (H, $r = -0.20$, $p = 0.58$, Pearson's linear correlation) in relation to NREM cumulative duration. Each dot represents the average synchrony from all single unit pairs recorded per session. Only significant linear regressions are plotted. See also [Figures S6](#), [S7](#), and [S12](#).

($p < 8.5 \times 10^{-10}$, [Figure 5B](#)), but not during REM sleep ($p = 0.4$). We reasoned that object cells might exhibit stronger reactivation during sleep following memory encoding, particularly during ripples. Indeed, we found significantly stronger recruitment of object cells during sleep oscillations, including slow wave activity ($p < 6.1 \times 10^{-4}$, [Figure 5C](#)), spindles ($p < 6.4 \times 10^{-3}$, [Figure 5D](#)), and ripple episodes ($p < 1.6 \times 10^{-3}$, [Figure 5E](#)), when compared to non-encoding neurons. This result suggests larger excitability and synchrony for task-engaged cells during sleep, thus supporting the consolidation model.

Next, we studied the transformation of the hippocampal spatial map during the task. Since we recorded neuronal spiking activity during the entire experimental session (i.e., sample, rest, and test phases), we were able to distinguish place cells, by establishing their place fields during spatial exploration of the task arena ([Figure 6A](#)), from non-spatial cells, by their negligible spatial information content ([Figure 6B](#)). We reasoned that place cells might be more strongly recruited during environment exploration than non-spatial cells due to their active engagement in spatial representation.⁵² Indeed, the firing rate of place cells was consistently higher than of non-spatial cells during all experimental task phases ([Figure 6C](#)) and, particularly, during NREM ([Figure 6D](#)). In a second step, we calculated the crosscorrelogram between either place cells or non-spatial cells and found that place cells were significantly more synchronized, in terms of peak crosscorrelation coefficients, than non-spatial cells during all task phases, with this difference being most pronounced during sleep ([Figure 6E](#)). Importantly, within sleep, the difference in peak crosscorrelations between place and non-spatial cells was much larger during NREM, when memory reactivations are assumed to take place than during REM sleep ([Figure 6F](#)). The activity and synchrony of interneurons displayed a pattern very similar to that of place cells during the task and sleep ([Figure S9](#)). Pairwise crosscorrelations confirmed that place cells were overall more synchronized than non-spatial cells across NREM ($p = 3.8 \times 10^{-89}$, [Figure 6G](#)). Finally, an analysis concentrating on firing during the respective brain oscillatory events showed that place cells were consistently more active than non-spatial cells for all event types, i.e., ripples, spindles, and slow wave activity ($p < 10^{-6}$, [Figures 6H–6J](#)).

We next studied how changes in the spatial configuration of the objects introduced with the retrieval period of the OPR, affected the spatial representations formed during the OPR encoding period. We assessed this by calculating the spatial correlation of place fields between encoding and retrieval phases of the OPR ([Figure 7A](#)). We found a distinct negative linear regression between the spatial correlation of place cells and NREM cumulative duration ($p = 0.03$, [Figure 7B](#)). That is, when the object configuration changed at retrieval testing, the location of place fields became segregated, leading to a reduced correlation between encoding and retrieval phases as NREM progressed, suggesting that NREM promoted place field remapping under these experimental conditions.^{53,54} Indeed, a variable

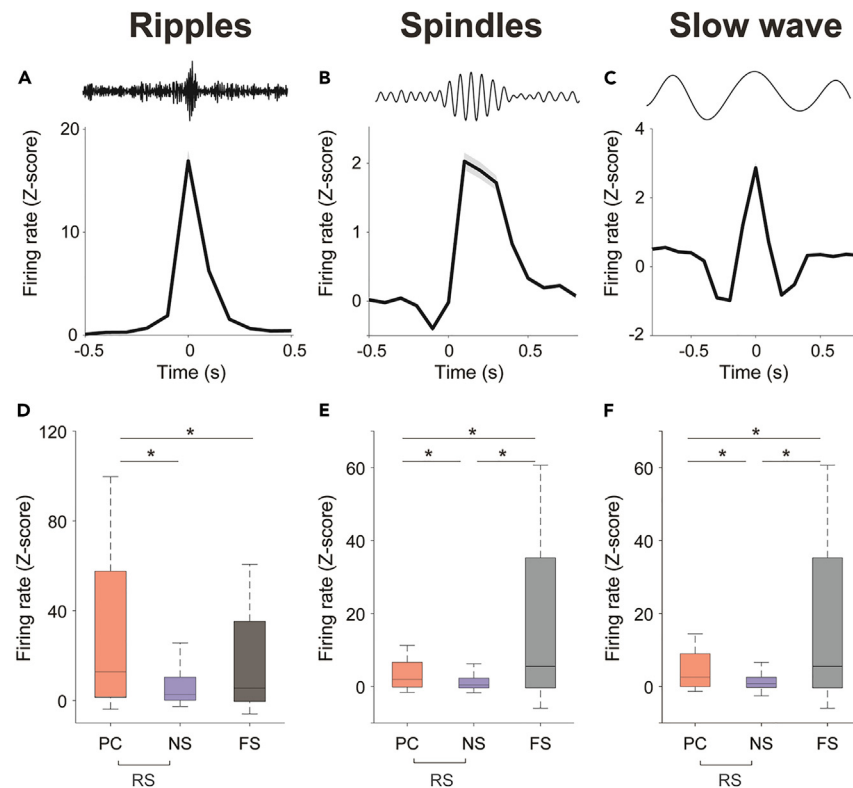


Figure 4. Hippocampal neuronal excitability is modulated by sleep oscillations

(A–C) Average normalized peri-event crosscorrelogram between cortical oscillations and dorsal CA1 single-unit activity ($n = 612$) across sleep sessions ($n = 16$). Top traces depict individual examples from filtered LFP traces.

(D–F) Boxplots depict peri-event crosscorrelogram peak amplitude between hippocampal cell activity and cortical oscillations across NREM. D, $p = 2.1 \times 10e-7$; E, $p = 1.8 \times 10e-10$; F, $p = 1.4 \times 10e-9$; Kruskal-Wallis test. * indicates $p < 0.005$, Wilcoxon ranked sum test. PC, place cells ($n = 192$); NS, non-spatial cells ($n = 324$); RS, regular spiking cells; FS, fast spiking cells ($n = 97$). See also [Figure S8](#).

proportion of place cells underwent global remapping such that their place fields at OPR encoding was faded away at the retrieval phase and, vice versa, cells without place field at encoding formed novel place fields at retrieval. Interestingly, the proportion of cells with changing place fields (either losing or gaining place fields between task phases) was proportional to the time spent in NREM, but not REM sleep, during the intervening sleep interval ([Figure S10](#)). Place cells are sensitive to mapping space in conjunction with spatial cues including objects.⁵⁵ Thus, rather than resulting from an updating of representations formed during OPR encoding upon exposure to the change in the object configuration at the retrieval phase, increased remapping of place cells at the retrieval phase, the increased place cell remapping at OPR retrieval might simply reflect a time-related instability of spatial representations.⁵⁵ To explore this alternative, we recorded hippocampal spiking from the same group of rats in an open field condition, i.e., using the same task arenas devoid of the objects ([Figure 7C](#)). We found that in the absence of objects, the spatial correlation of place fields was stable and independent of NREM ([Figure 7D](#)). Indeed, comparing directly the OPR and open field conditions showed that the significant negative correlation between the spatial correlation and NREM duration detected for the OPR condition also significantly differed from the respective correlation coefficient in the open field control condition ($p < 2.5 \times 10e-9$, bootstrapping, 1,000 iterations). Taken together, these results indicate that the time spent in NREM predicts the extent to which existing hippocampal spatial representations are decorrelated upon exposure to spatial novelty, i.e., a change in the spatial configuration.

We also found a decorrelating influence of NREM on the hippocampal representation of spatial locations when we assessed firing activity at the population level, rather than for single units.⁵⁴ For this, a map stability index was calculated by computing for each ensemble of simultaneously recorded neurons, the mean correlation coefficient between the encoding and retrieval phase of the OPR across all arena pixels.⁵⁶ In this way, the stability index provided an estimation of the persistence of the spatial ensemble representations across the two OPR task phases for each recording session (see [Figure 7E](#) for examples). Consistent with our findings for individual cells, we found that the stability index was negatively correlated with NREM duration, i.e., it decreased with increasing time an animal spent in NREM ($p = 0.028$, [Figure 7F](#)). For comparison, we also computed the stability index for the open field control condition (devoid of arena objects; [Figure 7G](#)). As found for the analyses of single units, the stability index in the open field condition was uncorrelated with NREM duration ([Figure 7H](#)). Indeed, a direct comparison between the OPR and open field conditions revealed that the significant negative correlation between the stability index and

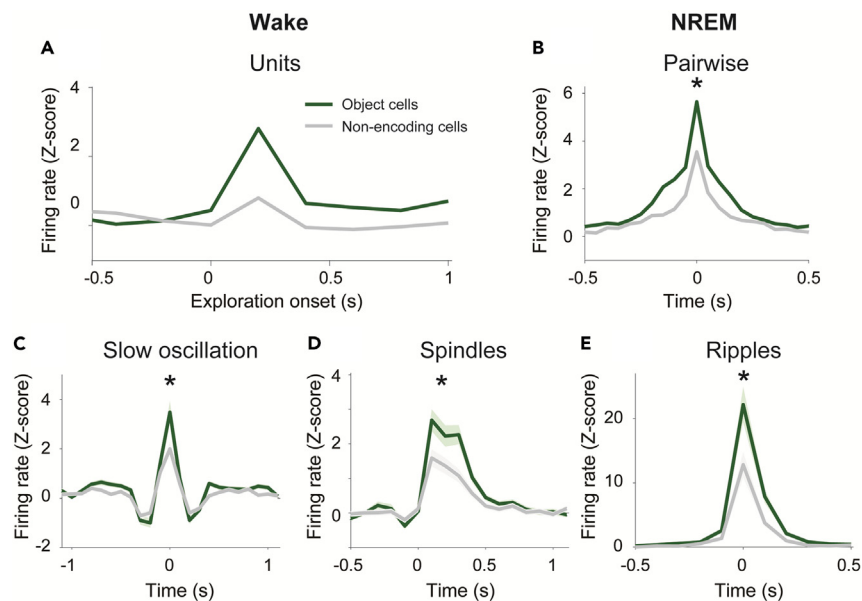


Figure 5. Hippocampal neuronal activity represents object exploration during OPR task

(A) Normalized firing rate of hippocampal single-units in relation to object exploration in the sample phase of the OPR task. Units increasing their firing rate over 2 SD for at least 200 ms from object exploration onset (time 0) were classified as activated neurons (object cells, $n = 114$). The remaining non-encoding neuronal population did not significantly change its firing rate in relation to object exploration ($n = 136$).

(B) Average pairwise crosscorrelograms between object cells (red, $n = 353$ pairs) and non-encoding neurons (black, $n = 812$ pairs). Synchrony between object cells was significantly larger ($p < 8.5 \times 10^{-10}$, Wilcoxon rank-sum test). Average peri-event crosscorrelograms between hippocampal units and sleep oscillations showing consistent differences between object cells and non-encoding cells: slow wave activity (C, $p < 6.1 \times 10^{-4}$), spindles (D, $p < 6.4 \times 10^{-3}$) and ripples (E, $p < 1.6 \times 10^{-3}$). Wilcoxon rank-sum test.

NREM duration obtained in the OPR condition also significantly differed from the respective correlation coefficient in the open field control condition ($p < 1.7 \times 10^{-14}$, bootstrapping, 1,000 iterations).

Finally, based on the significant correlations we observed between NREM duration and both spatial decorrelation and memory performance, we also examined whether the spatial decorrelation of place cells predicted OPR memory performance. This analysis revealed significant negative correlations ($p = 0.0128$ for single neurons, $p = 0.016$ for the stability index) indicating that the less stable representations were, the better OPR memory performance was at retrieval testing. A mediation analysis showed that the relationship between NREM and memory performance was direct ($P = 2 \times 10^{-16}$), and not mediated by spatial decorrelation. Overall, our results suggest that, in addition to the critical role exerted in memory performance, NREM actively supports the decorrelation of hippocampal spatial representations.

DISCUSSION

By recording hippocampal neuronal activity during spatial exploration and memory formation, we establish that sleep, and specifically the duration of NREM, is positively associated with both improved memory consolidation and destabilization of spatial representations. Indeed, spatial mapping as indicated by both activity of single-cells and neuronal populations became increasingly uncorrelated as NREM evolved, yet only upon exposure to a change in the spatial object configuration of the OPR task. Consistent with a role of sleep in homeostatic regulation of neuronal activity, we detected a progressive downscaling effect in the hippocampus, whereby brain oscillations including hippocampal ripples in parallel with neuronal firing rates progressively decreased across sleep. Despite downscaling, some episodic representations seemed to be retained, and possibly strengthened, as cells active during object exploration as well as cells forming a place field during OPR encoding consistently maintained their activity and synchrony during NREM, without a decrease. These cells reactivated during ripples in subsequent NREM, and exhibited stronger synchrony than the remaining neuronal population across sleep. Ripple-associated excitatory activity increased in relation to local inhibition, possibly supporting local synaptic plasticity in these circuits. On the other hand, synapses are known to be depressed by hippocampal ripples,⁵⁷ rendering these events a potential mechanism producing instability and decorrelated spatial representations upon spatial configurational changes in the OPR task.

Our experiments demonstrate that the effect of sleep on memory is cumulative and continuous, rather than discreet. Here, we used hippocampus recordings in combination with video monitoring for sleep scoring. Even though this is not the gold standard in the field, and could be considered to lead to incorrect scoring, it has been previously used and validated in the literature.^{27,41,58} Abundant evidence supports an active role for sleep in memory consolidation.^{59–62} Even short periods of sleep (1.5 h) favor the retention of a spatial context, and this has been consistently confirmed, for example, with the use of the OPR task.^{37,42,55} Indeed, immediate post-training sleep seems to be crucial for

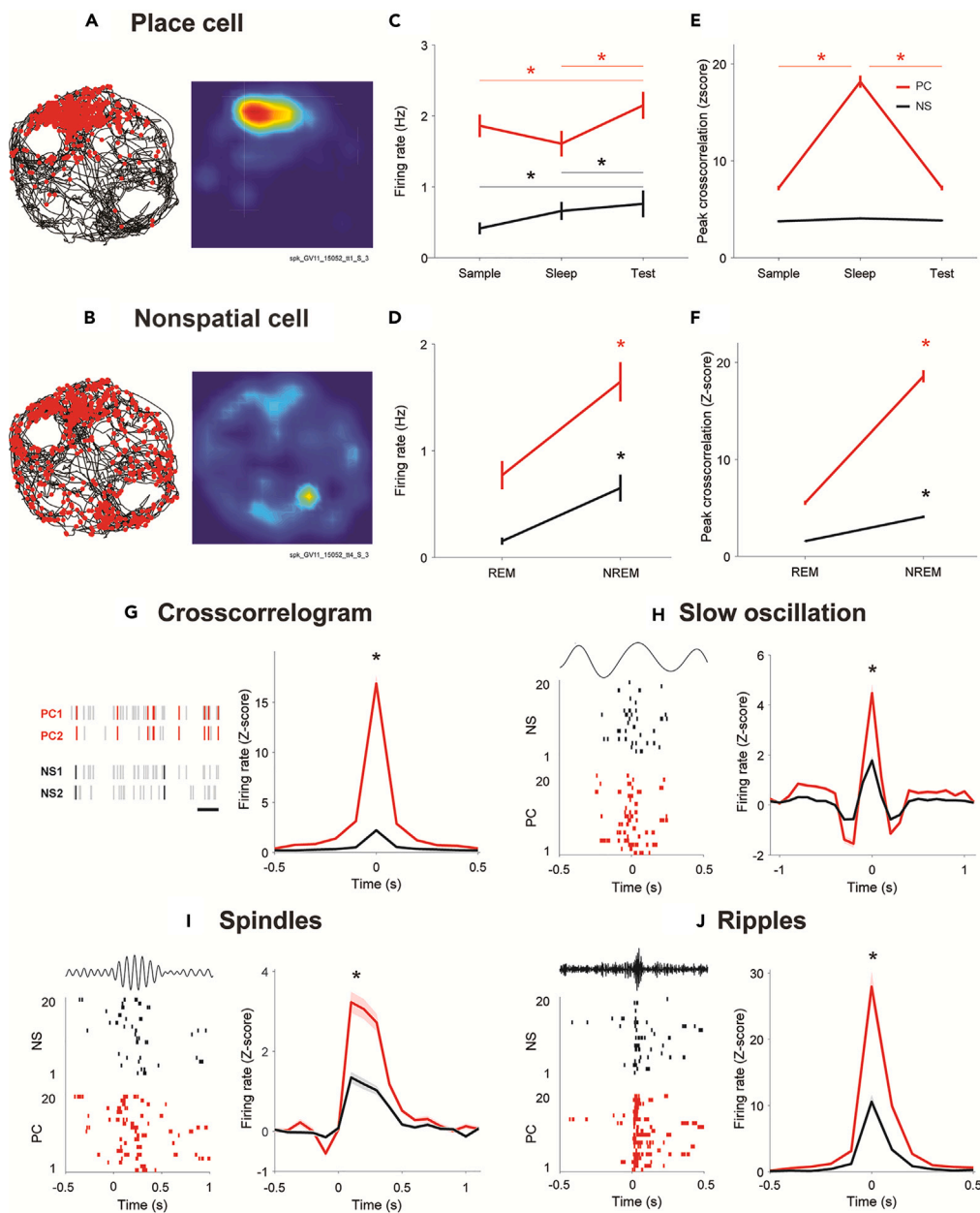


Figure 6. Place cells are more excitable and synchronized than non-spatial neurons during sleep

(A and B) Example place cell (A) and non-spatial cell (B) simultaneously recorded in the same experimental session, during the test phase (rat GV11, session 03). Left, spatial trajectory (black) and single spikes (red) discharged during arena exploration. Large white circles depict object location. Right, heat maps.

(C) Average firing rates of place cells (PC, $n = 192$) and non-spatial cells (NS, $n = 324$) according to task phase. Note place cells are consistently more active than non-spatial cells (two-way ANOVA, $p = 3.7 \times 10^{-21}$). Task stages were also different within groups (Kruskal-Wallis test, $p = 4.9 \times 10^{-9}$ for place cells and $p = 1.4 \times 10^{-6}$ for non-spatial cells).

(D) Average firing rates of place cells and non-spatial cells according to sleep phase. Note place cells are consistently more active than non-spatial cells (two-way ANOVA, $p = 3.1 \times 10^{-10}$). Sleep phases were also different within groups (Wilcoxon signed rank test, $p = 1.37 \times 10^{-10}$ for place cells and $p = 6.6 \times 10^{-8}$ for non-spatial cells).

(E) Peak pairwise crosscorrelation amplitude for place cells and non-spatial cells according to task phase. Note place cells are consistently more synchronized than non-spatial cells, particularly during sleep (Kruskal-Wallis test, $p = 4.8 \times 10^{-26}$ for place cells and $p = 0.20$ for non-spatial cells).

(F) Peak pairwise crosscorrelation amplitude for place cells and non-spatial cells according to sleep phase. Note place cells are consistently more synchronized than non-spatial cells (two-way ANOVA, $p = 1.8 \times 10^{-167}$), particularly during NREM. Sleep phases were also different within groups (Wilcoxon rank-sum test, $p = 7.9 \times 10^{-26}$ for place cells and $p = 4.5 \times 10^{-33}$ for non-spatial cells).

Figure 6. Continued

(G) Average pairwise crosscorrelograms between place cells (red, $n = 1,503$ pairs) and non-spatial neurons (black, $n = 4,221$ pairs). Synchrony between place cells was significantly larger (Wilcoxon rank-sum test, $p = 3.8 \times 10e-89$). Average peri-event crosscorrelogram between hippocampal units and sleep oscillations showing consistent differences between place cells and non-spatial cells: slow wave activity (H, $p = 2.3 \times 10e-7$), spindles (I, $p = 1.6 \times 10e-7$), and ripples (J, $p = 4.1 \times 10e-8$). Wilcoxon rank-sum test. Asterisks indicate significant differences, $p < 0.05$, pairwise Tukey's test. See also [Figures S9](#) and [S10](#).

memory consolidation, and optimal performance is reached when the retention interval takes place during the inactive light phase and animals are allowed to freely sleep,³⁷ whereas memory formation is disrupted following post-training sleep deprivation.^{38,63,64} Moreover, deeper sleep (i.e., enriched in NREM) reinforces spatial memory in the OPR task, and results in long-term memory that can last up to a week.⁴⁴ In this vein, our results further confirm that memory consolidation is not discreet, but gradual, and directly proportional to the cumulative time spent in NREM.^{43,44} Importantly, our experimental design omitted a pre-task sleep period, which would have served as a control. If included, the duration of pre-task NREM would also need to be factored into the analysis. Therefore, while the correlations we identified are significant and indicative, they alone do not definitively establish that the observed effects are exclusively linked to spatial memory. This aspect will need to be further explored in future experiments.

Thalamocortical oscillations like slow waves and spindles in conjunction with hippocampal ripples are tightly connected with memory consolidation.^{65,66} Indeed, communication between the hippocampus and neocortical circuits is regulated by sleep cardinal oscillations,^{14,18,67} and their temporal coordination enables the consolidation of labile memory traces.⁸ Hippocampal ripples coincide with neuronal reactivation of newly encoded memory traces, and the suppression of ripple episodes impairs spatial memory formation.^{9,68} Moreover, it has been reported that both ripples and spindles are enhanced during early post-training sleep in hippocampus-dependent memory tasks.^{69,70} Hence, ripple and spindle activity during early sleep following OPR encoding might indicate increased processing of the newly encoded spatial information.⁴⁴ On the other hand, our experiments revealed a general decrease in power and density of cortical and hippocampal oscillations across sleep, after animals acquired hippocampus-dependent spatial memory. There was in parallel a general decrease in neuronal firing activity with both parameters significantly depending on the time spent in NREM. Hence, rather than processing of specific memory, such general decreases are more likely to reflect a role of sleep, and specifically of NREM, in the homeostatic regulation of neuronal activity, as it has been previously described mainly for neocortical activity.²⁴

Significant evidence has accumulated in recent years pointing to early periods of sleep after encoding as critical for long-term memory formation.⁴⁴ The hippocampal replay of newly encoded memory appears to occur most frequently during early stages of sleep following memory encoding.^{71–73} Strengthening the coordination between the three different types of brain oscillatory event by electrical or optogenetic stimulation significantly improved spatial memory performance tested on the next day in the OPR task.^{8,74} Sleep spindle and ripple activity after encoding of a hippocampus-dependent odor-place association task was elevated for up to 2 h after post-encoding sleep onset.^{69,70} Consolidation of item memory, such as novel object recognition memory, likewise depends on early stages of sleep and integrity of hippocampal circuits.³⁸ Here, we revealed robust changes in neuronal spiking reactivating object and place encoding prior to sleep in relatively short periods of less than 90 min of sleep, aligned with what has been previously reported for much longer periods of sleep recordings.²⁴ Overall, even short periods of sleep immediately following waking experience are enough to trigger and sustain long-term memory formation, suggesting that our findings can be reasonably extrapolated to cases of long-term memory formation.

Of the three main brain states (waking, NREM, and REM), only REM sleep appears to be associated with a decrease in firing rates in the hippocampus.⁷⁵ We here replicated this observation, and moreover revealed that this REM sleep related drop in firing activity is larger for non-spatial cells than for place cells. It is presently unclear whether this pattern is specific to the hippocampus or likewise found in the neocortex. Electrical recordings in neocortex revealed continuously high firing activity²⁴ whereas *in vivo* calcium imaging revealed a drop in neocortical activity during REM sleep that was restricted to the pyramidal cells and which, similar to the present findings in the hippocampus, was less pronounced for cells putatively involved in prior encoding.^{76,77} Nevertheless, network regulation during REM sleep might essentially differ, e.g., due to local effects of circulating neuromodulators. Indeed, active navigation and exploration during wakefulness implies high levels of acetylcholine, serotonin, histamine, and noradrenaline in the hippocampus, whereas during REM sleep only the cholinergic tone remains elevated.⁷⁸ Further, hippocampal multiple unit recordings revealed negligible changes in global firing rates during sleep following exploration of a novel environment exploration^{73,79} or after electrically induced LTP,⁸⁰ suggesting that hippocampal firing rates at a global level are relatively stable across learning and brain states.^{52,81,82} Simultaneously, such observations have questioned the participation of the hippocampus in the homeostatic regulation of brain activity during sleep.²⁴ Yet, our findings of hippocampal oscillations and coordinated neuronal spiking decreasing across NREM strongly argue for an involvement of the hippocampus in such homeostasis.

The central finding of our study was that the time the rat spent in NREM did not only predict the rat's memory on the OPR test but, on the other hand, an increased instability of the hippocampal representations as indicated by an enhanced decorrelation of single cell place fields and the cell population vector activity at exposure to the changed object configuration during the OPR test phase. This finding was unexpected in light of evidence that the stability of place cells is important for memory maintenance.^{83,84} Previous experiments, however, showed that hippocampal cells expressing the early gene *c-fos*, a prominent genetic marker of neural activity associated with memory formation,⁸⁵ are more unstable than other neurons.⁸⁶ More recent findings have reinforced the idea that instability of place cells is important for memory updating, particularly upon spatial changes as those taking place in the OPR task.⁵⁵ Thus, a population of highly volatile place cells has been described, with strong tendency to remap during the OPR retrieval phase (49). These observations suggest that neuronal populations participating in memory processing exhibit varying degrees of flexibility in the encoding of spatial information, which is also consistent with our findings of adaptable spatial mapping contingent upon changes in the spatial configuration of the OPR objects. Sleep deprivation,

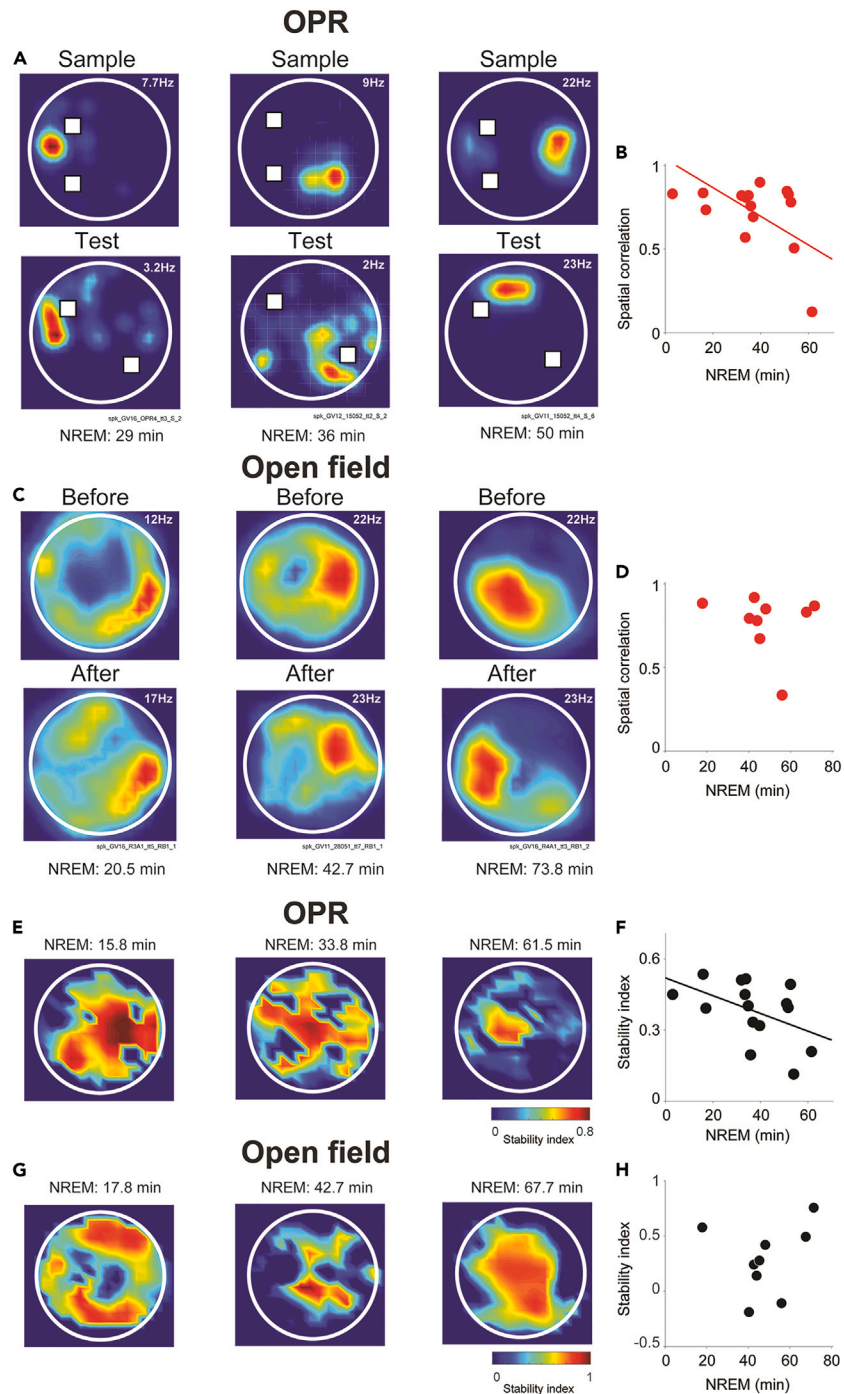


Figure 7. Stability of spatial representations decreases across sleep

Examples of place cells recorded in the exploration phases of the OPR task (A) or the open field (C). Average spatial correlation of place cells in relation to NREM duration for the OPR task (B, computed between test and sample phases, $r = -0.53$, $p = 0.03$, Spearman's correlation) or the open field (D, computed between after and before sleep, $r = 0.07$, $p = 0.97$, Spearman's correlation). Examples of population vector correlation maps obtained from sessions with different NREM durations for the OPR task (E, $n = 15$ sessions) and the open field (G, $n = 9$ sessions). Population vector correlation (stability index) in relation to NREM duration for the OPR task (F, $r = -0.55$, $p = 0.028$, Spearman's correlation) and open field (H, $r = 0.35$, $p = 0.36$, Spearman's correlation). Only significant linear regressions are plotted.

conversely, might interfere with memory consolidation by making hippocampal spatial representations more static and less flexible.⁵⁵ Interestingly, along this line of evidence, scarce remapping in response to environmental changes has been interpreted as possibly reflecting incomplete synaptic downscaling by preventing correct encoding of a new different object configuration. This idea receives further support by observations showing that place cell remapping involves plastic mechanisms associated with synaptic depression.⁸⁷ Also, short retention intervals (5 min) failed to induce place cell remapping,⁸⁸ and this is well comparable to our experiments where in the animals that slept for only very brief periods, hippocampal spatial representations remained highly correlated between encoding and retrieval testing.

At this point, it is reasonable to consider why better memory performance is linked to a higher degree of spatial decorrelation. How can retrieval of a spatial memory improve although its hippocampal representation loses stability with increasing time in NREM? Notably, our mediation analysis revealed the relation between the decorrelation of spatial firing activity and behavioral OPR performance not to be causal suggesting another factor present during NREM commonly driving both processes. A tempting speculation here refers to the ripples. Hippocampal ripples, on the one hand, can depotentiate excitatory synapses⁵⁷ thereby decorrelating hippocampal place cell networks and increasing their flexibility for encoding novel spatial information. Simultaneously, hippocampal ripples accompanying place cell reactivations are considered key to the transmission of reactivated memory information to extrahippocampal mainly neocortical sites.⁸⁹ This transmission might well be supported by a more general increase in the excitation/inhibition balance toward increased excitation in respective hippocampal networks, as observed here specifically in conjunction with ripple events. Ripples additionally coupling with thalamic spindles and neocortical slow waves, in this way, likely promote the long-term storage of the spatial information in neocortical networks.^{18,74,90} Indeed, there is growing evidence that consolidated memory from spatial conditions ultimately resides in the medial prefrontal cortex (e.g.,^{91,92}). Thus, ripples occurring during NREM might essentially contribute to this redistribution of the representations to medial prefrontal cortex, which are probably then also used to either reinstate in the hippocampus the original place fields in future encoding situation and, if necessary, upon significant spatial change, to support remapping.^{93,94}

Two theories have been proposed to account for the role of sleep in the consolidation of specific memories and in the global homeostatic regulation of excitatory synapses and firing activity, respectively.^{89,95} The 'active systems consolidation' model poses that neurons activated and encoding information during recent waking experience will remain selectively active during sleep, discharging mostly within hippocampal ripples and neocortical spindles.^{11,51,96–98} In support of this claim, the present experiments revealed a recurrent reactivation of cells active during object exploration and forming place fields during OPR encoding during subsequent sleep, with this reactivation being significantly larger than for the remaining population in our experiments. The synaptic homeostasis hypothesis proposes that waking experience due to the continuous encoding of information, increases the overall synaptic potentiation and, in turn, excitation of neuronal networks, so that sleep, particularly NREM, reduces and down-selects synaptic potentiation and firing rates.^{25,26,99} This prediction was also verified in our recordings, as the amplitude and synchrony of cortical and hippocampal oscillations as well as neuronal spiking in hippocampal networks progressively decreased the longer the time spent in NREM. Importantly, to also explain the consolidation of specific memory during sleep, the synaptic homeostasis hypothesis, as an additional mechanism, assumes that those cells participating in memory encoding during wakefulness are, to a certain extent, spared from subsequent synaptic renormalization processes, thereby providing a relative enhancement of memory information encoded in these synaptic ensembles.¹⁰⁰ Consonant with this prediction, we revealed the decrease in firing rate across sleep to be distinctly dampened for those cells engaging in the encoding of objects and place during the OPR encoding phase, and these cells also maintained stronger pairwise correlations and locking to sleep oscillations throughout the sleep period than the remaining neuronal population. Thus, our findings, in parallel, provide confirmatory support for both theories. Moreover, suggesting sharp-wave ripples as a mechanism possibly acting in both directions, i.e., to enhance spatial memory and to decorrelate spatial hippocampal representations, they provide first cues as to how these seemingly opposing functions might be established in the same hippocampal networks.

Limitations of the study

The main limitation of our study is that our experimental design omitted a pre-task sleep period, which would have served as a control to compared neuronal spiking activity. Therefore, while the correlations we identified are significant and indicative, they alone do not definitively establish that the observed effects are exclusively linked to spatial memory, as they can be related with sleep dynamics. This aspect will need to be further explored in future experiments.

STAR★METHODS

Detailed methods are provided in the online version of this paper and include the following:

- KEY RESOURCES TABLE
- RESOURCE AVAILABILITY
 - Lead contact
 - Materials availability
 - Data and code availability
- EXPERIMENTAL MODEL AND STUDY PARTICIPANT DETAILS
- METHODS DETAILS
 - Behavioral apparatus
 - Habituation

- Object-place recognition (OPR) task
- Task scoring and discrimination index
- Stereotaxic surgery for electrode implantation
- Electrophysiological recordings
- Histology and recording site identification
- Sleep scoring
- Sleep oscillations
- Spike sorting
- Place cells
- Peri-event cross-correlograms
- Population vector
- **QUANTIFICATION AND STATISTICAL ANALYSIS**
- Statistical analysis

SUPPLEMENTAL INFORMATION

Supplemental information can be found online at <https://doi.org/10.1016/j.isci.2024.110076>.

ACKNOWLEDGMENTS

This study was funded by ANID fondecyt 1230589 and ANID ANILLO ACT210053.

AUTHOR CONTRIBUTIONS

G.V. carried out experiments and analyzed data, N.E. analyzed data, A.L. carried out experiments, M.C. analyzed data, M.I. designed the research project, J.B. designed the research project and wrote the manuscript, P.F. carried out experiments, designed the research project, and wrote the manuscript.

DECLARATION OF INTERESTS

The authors declare no competing interests.

Received: October 16, 2023

Revised: February 2, 2024

Accepted: May 19, 2024

Published: May 22, 2024

REFERENCES

1. Abel, T., Havekes, R., Saletin, J.M., and Walker, M.P. (2013). Sleep, plasticity and memory from molecules to whole-brain networks. *Curr. Biol.* 23, R774–R788. <https://doi.org/10.1016/j.cub.2013.07.025>.
2. Rasch, B., and Born, J. (2013). About sleep's role in memory. *Physiol. Rev.* 93, 681–766. <https://doi.org/10.1152/PHYSREV.00032.2012>.
3. Stickgold, R., and Walker, M.P. (2013). Sleep-dependent memory triage: evolving generalization through selective processing. *Nat. Neurosci.* 16, 139–145. <https://doi.org/10.1038/NN.3303>.
4. Ttononi, G., and Cirelli, C. (2014). Sleep and the price of plasticity: from synaptic and cellular homeostasis to memory consolidation and integration. *Neuron* 81, 12–34. <https://doi.org/10.1016/j.neuron.2013.12.025>.
5. Gais, S., and Born, J. (2004). Declarative memory consolidation: mechanisms acting during human sleep. *Learn. Mem.* 11, 679–685. <https://doi.org/10.1101/LM.80504>.
6. Gais, S., Lucas, B., and Born, J. (2006). Sleep after learning aids memory recall. *Learn. Mem.* 13, 259–262. <https://doi.org/10.1101/LM.132106>.
7. Smith, C. (2001). Sleep states and memory processes in humans: procedural versus declarative memory systems. *Sleep Med. Rev.* 5, 491–506. <https://doi.org/10.1053/SMRV.2001.0164>.
8. Maingret, N., Girardeau, G., Todorova, R., Goutierre, M., and Zugaro, M. (2016). Hippocampo-cortical coupling mediates memory consolidation during sleep. *Nat. Neurosci.* 19, 959–964. <https://doi.org/10.1038/NN.4304>.
9. Girardeau, G., Benchenane, K., Wiener, S.I., Buzsáki, G., and Zugaro, M.B. (2009). Selective suppression of hippocampal ripples impairs spatial memory. *Nat. Neurosci.* 12, 1222–1223. <https://doi.org/10.1038/nn.2384>.
10. Wilson, M.A., and McNaughton, B.L. (1993). Dynamics of the hippocampal ensemble code for space. *Science* 261, 1055–1058. <https://doi.org/10.1126/SCIENCE.8351520>.
11. Stickgold, R. (2005). Sleep-dependent memory consolidation. *Nature* 437, 1272–1278. <https://doi.org/10.1038/NATURE04286>.
12. Born, J., and Wilhelm, I. (2012). System consolidation of memory during sleep. *Psychol. Res.* 76, 192–203. <https://doi.org/10.1007/S00426-011-0335-6>.
13. Rasch, B., Büchel, C., Gais, S., and Born, J. (2007). Odor cues during slow-wave sleep prompt declarative memory consolidation. *Science* 315, 1426–1429. <https://doi.org/10.1126/SCIENCE.1138581>.
14. Inostroza, M., and Born, J. (2013). Sleep for preserving and transforming episodic memory. *Annu. Rev. Neurosci.* 36, 79–102. <https://doi.org/10.1146/ANNUREV-NEURO-062012-170429>.
15. Ylinen, A., Bragin, A., Nádasdy, Z., Jandó, G., Szabó, I., Sik, A., and Buzsáki, G. (1995). Sharp wave-associated high-frequency oscillation (200 Hz) in the intact hippocampus: Network and intracellular mechanisms. *J. Neurosci.* 15, 30–46. <https://doi.org/10.1523/jneurosci.15-01-00030.1995>.
16. Steriade, M., Wyzinski, P., and Oakson, G. (1971). Activities in synaptic pathways between the motor cortex and ventrolateral thalamus underlying EEG spindle waves. *Int. J. Neurol.* 8, 211–229.
17. Steriade, M., Nuñez, A., and Amzica, F. (1993). A novel slow (< 1 Hz) oscillation of neocortical neurons in vivo: depolarizing and hyperpolarizing components. *J. Neurosci.* 13, 3252–3265. <https://doi.org/10.1523/JNEUROSCI.13-08-03252.1993>.

18. Staresina, B.P., Bergmann, T.O., Bonfond, M., van der Meij, R., Jensen, O., Deuker, L., Elger, C.E., Axmacher, N., and Fell, J. (2015). Hierarchical nesting of slow oscillations, spindles and ripples in the human hippocampus during sleep. *Nat. Neurosci.* 18, 1679–1686. <https://doi.org/10.1038/nn.4119>.
19. Isomura, Y., Sirota, A., Özen, S., Montgomery, S., Mizuseki, K., Henze, D.A., and Buzsáki, G. (2006). Integration and Segregation of Activity in Entorhinal-Hippocampal Subregions by Neocortical Slow Oscillations. *Neuron* 52, 871–882. <https://doi.org/10.1016/j.neuron.2006.10.023>.
20. Sirota, A., Csicsvari, J., Buhl, D., and Buzsáki, G. (2003). Communication between neocortex and hippocampus during sleep in rodents. *Proc. Natl. Acad. Sci. USA* 100, 2065–2069. <https://doi.org/10.1073/PNAS.0437938100>.
21. Steriade, M. (2006). Grouping of brain rhythms in corticothalamic systems. *Neuroscience* 137, 1087–1106. <https://doi.org/10.1016/j.neuroscience.2005.10.029>.
22. Logothetis, N.K., Eschenko, O., Murayama, Y., Augath, M., Steudel, T., Evrard, H.C., Besserve, M., and Oeltermann, A. (2012). Hippocampal-cortical interaction during periods of subcortical silence. *Nature* 491, 547–553. <https://doi.org/10.1038/nature11618>.
23. Vyazovskiy, V.V., Olcese, U., Hanlon, E.C., Nir, Y., Cirelli, C., and Tononi, G. (2011). Local sleep in awake rats. *Nature* 472, 443–447. <https://doi.org/10.1038/NATURE10009>.
24. Vyazovskiy, V.V., Olcese, U., Lazimy, Y.M., Faraguna, U., Esser, S.K., Williams, J.C., Cirelli, C., and Tononi, G. (2009). Cortical firing and sleep homeostasis. *Neuron* 63, 865–878. <https://doi.org/10.1016/j.NEURON.2009.08.024>.
25. Borbely, A.A. (1982). A two process model of sleep regulation. *Hum. Neurobiol.* 1, 195–204.
26. Tononi, G., and Cirelli, C. (2006). Sleep function and synaptic homeostasis. *Sleep Med. Rev.* 10, 49–62. <https://doi.org/10.1016/j.SMRV.2005.05.002>.
27. Grosmark, A.D., Mizuseki, K., Pastalkova, E., Diba, K., and Buzsáki, G. (2012). REM sleep reorganizes hippocampal excitability. *Neuron* 75, 1001–1007. <https://doi.org/10.1016/j.NEURON.2012.08.015>.
28. Niethard, N., Burgalossi, A., and Born, J. (2017). Plasticity during sleep is linked to specific regulation of cortical circuit activity. *Front. Neural Circuits* 11, 65. <https://doi.org/10.3389/FNCIR.2017.00065/BIBTEX>.
29. O’Keefe, J., and Dostrovsky, J. (1971). The hippocampus as a spatial map. Preliminary evidence from unit activity in the freely moving rat. *Brain Res.* 34, 171–175. [https://doi.org/10.1016/0006-8993\(71\)90358-1](https://doi.org/10.1016/0006-8993(71)90358-1).
30. Mizumori, S.J.Y. (2006). Hippocampal place fields: a neural code for episodic memory? *Hippocampus* 16, 685–690. <https://doi.org/10.1002/HIPO.20209>.
31. Smith, D.M., and Mizumori, S.J.Y. (2006). Hippocampal place cells, context, and episodic memory. *Hippocampus* 16, 716–729. <https://doi.org/10.1002/HIPO.20208>.
32. Muller, R.U., and Kubie, J.L. (1987). The effects of changes in the environment on the spatial firing of hippocampal complex-spike cells. *J. Neurosci.* 7, 1951–1968. <https://doi.org/10.1523/JNEUROSCI.07-07-01951.1987>.
33. Lever, C., Wills, T., Cacucci, F., Burgess, N., and O’Keefe, J. (2002). Long-term plasticity in hippocampal place-cell representation of environmental geometry. *Nature* 416, 90–94. <https://doi.org/10.1038/416090A>.
34. Knierim, J.J., Kudrimoti, H.S., and McNaughton, B.L. (1995). Place cells, head direction cells, and the learning of landmark stability. *J. Neurosci.* 15, 1648–1659. <https://doi.org/10.1523/JNEUROSCI.15-03-01648.1995>.
35. Sharp, P.E., Kubie, J.L., and Muller, R.U. (1990). Firing properties of hippocampal neurons in a visually symmetrical environment: contributions of multiple sensory cues and mnemonic processes. *J. Neurosci.* 10, 3093–3105. <https://doi.org/10.1523/JNEUROSCI.10-09-03093.1990>.
36. Shapiro, M.L., Tanila, H., and Eichenbaum, H. (1997). Cues that hippocampal place cells encode: dynamic and hierarchical representation of local and distal stimuli. *Hippocampus* 7, 624–642. [https://doi.org/10.1002/\(sici\)1098-1063\(1997\)7:6<624::aid-hipo5>3.0.co;2-e](https://doi.org/10.1002/(sici)1098-1063(1997)7:6<624::aid-hipo5>3.0.co;2-e).
37. Binder, S., Baier, P.C., Mölle, M., Inostroza, M., Born, J., and Marshall, L. (2012). Sleep enhances memory consolidation in the hippocampus-dependent object-place recognition task in rats. *Neurobiol. Learn. Mem.* 97, 213–219. <https://doi.org/10.1016/J.NLM.2011.12.004>.
38. Sawangjit, A., Oyanedel, C.N., Niethard, N., Salazar, C., Born, J., and Inostroza, M. (2018). The hippocampus is crucial for forming non-hippocampal long-term memory during sleep. *Nature* 564, 109–113. <https://doi.org/10.1038/S41586-018-0716-8>.
39. Kelemen, E., Bahrendt, M., Born, J., and Inostroza, M. (2014). Hippocampal Corticosterone Impairs Memory Consolidation During Sleep but Improves Consolidation in the Wake State. *Hippocampus* 24, 510–515. <https://doi.org/10.1002/hipo.22266>.
40. Inostroza, M., and Born, J. (2013). Sleep for preserving and transforming episodic memory. *Annu. Rev. Neurosci.* 36, 79–102. <https://doi.org/10.1146/annurev-neuro-062012-170429>.
41. Peyrache, A., Lacroix, M.M., Petersen, P.C., and Buzsáki, G. (2015). Internally organized mechanisms of the head direction sense. *Nat. Neurosci.* 18, 569–575. <https://doi.org/10.1038/NN.3968>.
42. Inostroza, M., Binder, S., and Born, J. (2013). Sleep-dependency of episodic-like memory consolidation in rats. *Behav. Brain Res.* 237, 15–22. <https://doi.org/10.1016/J.BBR.2012.09.011>.
43. Diekelmann, S., Biggel, S., Rasch, B., and Born, J. (2012). Offline consolidation of memory varies with time in slow wave sleep and can be accelerated by cuing memory reactivations. *Neurobiol. Learn. Mem.* 98, 103–111. <https://doi.org/10.1016/J.NLM.2012.07.002>.
44. Sawangjit, A., Oyanedel, C.N., Niethard, N., Born, J., and Inostroza, M. (2020). Deepened sleep makes hippocampal spatial memory more persistent. *Neurobiol. Learn. Mem.* 173, 107245. <https://doi.org/10.1016/J.NLM.2020.107245>.
45. Kim, J., Gulati, T., and Ganguly, K. (2019). Competing Roles of Slow Oscillations and Delta Waves in Memory Consolidation versus Forgetting. *Cell* 179, 514–526.e13. <https://doi.org/10.1016/J.CELL.2019.08.040>.
46. Markram, H., Lübke, J., Frotscher, M., and Sakmann, B. (1997). Regulation of synaptic efficacy by coincidence of postsynaptic APs and EPSPs. *Science* 275, 213–215. <https://doi.org/10.1126/science.275.5297.213>.
47. Miyawaki, H., Watson, B.O., and Diba, K. (2019). Neuronal firing rates diverge during REM and homogenize during non-REM. *Sci. Rep.* 9, 689. <https://doi.org/10.1038/S41598-018-36710-8>.
48. Miyawaki, H., and Diba, K. (2016). Regulation of Hippocampal Firing by Network Oscillations during Sleep. *Curr. Biol.* 26, 893–902. <https://doi.org/10.1016/J.CUB.2016.02.024>.
49. Watson, B.O., Levenstein, D., Greene, J.P., Gelinias, J.N., and Buzsáki, G. (2016). Network Homeostasis and State Dynamics of Neocortical Sleep. *Neuron* 90, 839–852. <https://doi.org/10.1016/J.NEURON.2016.03.036>.
50. Lobato, I.N., Aleman-Zapata, A., Samanta, A., Bogers, M., Narayanan, S., Rayan, A., Alonso, A., van der Meij, J., Khamassi, M., Khan, Z.U., et al. (2023). Increased cortical plasticity leads to memory interference and enhanced hippocampal-cortical interactions. *Elife* 12, e84911. <https://doi.org/10.7554/ELIFE.84911>.
51. Buzsáki, G. (1989). Two-stage model of memory trace formation: a role for “noisy” brain states. *Neuroscience* 31, 551–570. [https://doi.org/10.1016/0306-4522\(89\)90423-5](https://doi.org/10.1016/0306-4522(89)90423-5).
52. Pavlides, C., and Winson, J. (1989). Influences of hippocampal place cell firing in the awake state on the activity of these cells during subsequent sleep episodes. *J. Neurosci.* 9, 2907–2918. <https://doi.org/10.1523/JNEUROSCI.09-08-02907.1989>.
53. Fyhn, M., Hafting, T., Treves, A., Moser, M.B., and Moser, E.I. (2007). Hippocampal remapping and grid realignment in entorhinal cortex. *Nature* 446, 190–194. <https://doi.org/10.1038/NATURE05601>.
54. Leutgeb, S., Leutgeb, J.K., Barnes, C.A., Moser, E.I., McNaughton, B.L., and Moser, M.B. (2005). Independent codes for spatial and episodic memory in hippocampal neuronal ensembles. *Science* 309, 619–623. <https://doi.org/10.1126/SCIENCE.1114037>.
55. Yuan, R.K., Lopez, M.R., Ramos-Alvarez, M.-M., Normandin, M.E., Thomas, A.S., Uygun, D.S., Cerda, V.R., Grenier, A.E., Wood, M.T., Gagliardi, C.M., et al. (2021). Differential effect of sleep deprivation on place cell representations, sleep architecture, and memory in young and old mice. *Cell Rep.* 35, 109234. <https://doi.org/10.1016/j.celrep.2021.109234>.
56. Roux, L., Hu, B., Eichler, R., Stark, E., and Buzsáki, G. (2017). Sharp wave ripples during learning stabilize the hippocampal spatial map. *Nat. Neurosci.* 20, 845–853. <https://doi.org/10.1038/nn.4543>.
57. Norimoto, H., Makino, K., Gao, M., Shikano, Y., Okamoto, K., Ishikawa, T., Sasaki, T., Hioki, H., Fujisawa, S., and Ikegaya, Y. (2018). Hippocampal ripples down-regulate synapses. *Science* 359, 1524–1527. https://doi.org/10.1126/SCIENCE.AAO0702/SUPPL_FILE/AAO0702_NORIMOTO_SM_REVISION.1.PDF.
58. Shin, J.D., and Jadhav, S.P. (2023). Cortical ripples mediate top-down suppression of hippocampal reactivation during sleep

- memory consolidation. Preprint at bioRxiv. <https://doi.org/10.1101/2023.12.12.571373>.
59. Born, J., Rasch, B., and Gais, S. (2006). Sleep to remember. *Neuroscientist* 12, 410–424. <https://doi.org/10.1177/1073858406292647>.
 60. Diekelmann, S., and Born, J. (2010). The memory function of sleep. *Nat. Rev. Neurosci.* 11, 114–126. <https://doi.org/10.1038/NRN2762>.
 61. Payne, J.D., and Kensinger, E.A. (2011). Sleep leads to changes in the emotional memory trace: evidence from fMRI. *J. Cogn. Neurosci.* 23, 1285–1297. <https://doi.org/10.1162/JOCN.2010.21526>.
 62. Lewis, P.A., and Durrant, S.J. (2011). Overlapping memory replay during sleep builds cognitive schemata. *Trends Cogn. Sci.* 15, 343–351. <https://doi.org/10.1016/J.TICS.2011.06.004>.
 63. Havekes, R., Bruinenberg, V.M., Tudor, J.C., Ferri, S.L., Baumann, A., Meerlo, P., and Abel, T. (2014). Transiently increasing cAMP levels selectively in hippocampal excitatory neurons during sleep deprivation prevents memory deficits caused by sleep loss. *J. Neurosci.* 34, 15715–15721. <https://doi.org/10.1523/JNEUROSCI.2403-14.2014>.
 64. Prince, T.M., Wimmer, M., Choi, J., Havekes, R., Aton, S., and Abel, T. (2014). Sleep deprivation during a specific 3-hour time window post-training impairs hippocampal synaptic plasticity and memory. *Neurobiol. Learn. Mem.* 109, 122–130. <https://doi.org/10.1016/J.NLM.2013.11.021>.
 65. Ulrich, D. (2016). Sleep Spindles as Facilitators of Memory Formation and Learning. *Neural Plast.* 2016, 1796715. <https://doi.org/10.1155/2016/1796715>.
 66. Antony, J.W., Schönauer, M., Staresina, B.P., and Cairney, S.A. (2019). Sleep Spindles and Memory Reprocessing. *Trends Neurosci.* 42, 1–3. <https://doi.org/10.1016/J.TINS.2018.09.012>.
 67. Girardeau, G., and Lopes-Dos-Santos, V. (2021). Brain neural patterns and the memory function of sleep. *Science* 374, 560–564. <https://doi.org/10.1126/SCIENCE.AB18370>.
 68. Ego-Stengel, V., and Wilson, M.A. (2010). Disruption of ripple-associated hippocampal activity during rest impairs spatial learning in the rat. *Hippocampus* 20, 1–10. <https://doi.org/10.1002/HIPO.20707>.
 69. Eschenko, O., Mölle, M., Born, J., and Sara, S.J. (2006). Elevated sleep spindle density after learning or after retrieval in rats. *J. Neurosci.* 26, 12914–12920. <https://doi.org/10.1523/JNEUROSCI.3175-06.2006>.
 70. Eschenko, O., Ramadan, W., Mölle, M., Born, J., and Sara, S.J. (2008). Sustained increase in hippocampal sharp-wave ripple activity during slow-wave sleep after learning. *Learn. Mem.* 15, 222–228. <https://doi.org/10.1101/LM.726008>.
 71. O'Neill, J., Pleydell-Bouverie, B., Dupret, D., and Csicsvari, J. (2010). Play it again: reactivation of waking experience and memory. *Trends Neurosci.* 33, 220–229. <https://doi.org/10.1016/J.TINS.2010.01.006>.
 72. Giri, B., Miyawaki, H., Mizuseki, K., Cheng, S., and Diba, K. (2019). Hippocampal Reactivation Extends for Several Hours Following Novel Experience. *J. Neurosci.* 39, 866–875. <https://doi.org/10.1523/JNEUROSCI.1950-18.2018>.
 73. Kudrimoti, H.S., Barnes, C.A., and McNaughton, B.L. (1999). Reactivation of hippocampal cell assemblies: effects of behavioral state, experience, and EEG dynamics. *J. Neurosci.* 19, 4090–4101. <https://doi.org/10.1523/JNEUROSCI.19-10-04090.1999>.
 74. Latchoumane, C.F.V., Ngo, H.V.V., Born, J., and Shin, H.S. (2017). Thalamic Spindles Promote Memory Formation during Sleep through Triple Phase-Locking of Cortical, Thalamic, and Hippocampal Rhythms. *Neuron* 95, 424–435.e6. <https://doi.org/10.1016/J.NEURON.2017.06.025>.
 75. Montgomery, S.M., Sirota, A., and Buzsáki, G. (2008). Theta and gamma coordination of hippocampal networks during waking and rapid eye movement sleep. *J. Neurosci.* 28, 6731–6741. <https://doi.org/10.1523/JNEUROSCI.1227-08.2008>.
 76. Niethard, N., Brodt, S., and Born, J. (2021). Cell-Type-Specific Dynamics of Calcium Activity in Cortical Circuits over the Course of Slow-Wave Sleep and Rapid Eye Movement Sleep. *J. Neurosci.* 41, 4212–4222. <https://doi.org/10.1523/JNEUROSCI.1957-20.2021>.
 77. Niethard, N., Hasegawa, M., Itokazu, T., Oyanedel, C.N., Born, J., and Sato, T.R. (2016). Sleep-Stage-Specific Regulation of Cortical Excitation and Inhibition. *Curr. Biol.* 26, 2739–2749. <https://doi.org/10.1016/J.CUB.2016.08.035>.
 78. Steriade, M. (2004). Acetylcholine systems and rhythmic activities during the waking-sleep cycle. *Prog. Brain Res.* 145, 179–196. [https://doi.org/10.1016/S0079-6123\(03\)45013-9](https://doi.org/10.1016/S0079-6123(03)45013-9).
 79. Hirase, H., Leinekugel, X., Czurkó, A., Csicsvari, J., and Buzsáki, G. (2001). Firing rates of hippocampal neurons are preserved during subsequent sleep episodes and modified by novel awake experience. *Proc. Natl. Acad. Sci. USA* 98, 9386–9390. <https://doi.org/10.1073/PNAS.161274398>.
 80. Dragoi, G., Harris, K.D., and Buzsáki, G. (2003). Place representation within hippocampal networks is modified by long-term potentiation. *Neuron* 39, 843–853. [https://doi.org/10.1016/S0896-6273\(03\)00465-3](https://doi.org/10.1016/S0896-6273(03)00465-3).
 81. Karlsson, M.P., and Frank, L.M. (2008). Network dynamics underlying the formation of sparse, informative representations in the hippocampus. *J. Neurosci.* 28, 14271–14281. <https://doi.org/10.1523/JNEUROSCI.4261-08.2008>.
 82. Buzsáki, G., Kaila, K., and Raichle, M. (2007). Inhibition and brain work. *Neuron* 56, 771–783. <https://doi.org/10.1016/J.NEURON.2007.11.008>.
 83. Kentros, C.G., Agnihotri, N.T., Streater, S., Hawkins, R.D., and Kandel, E.R. (2004). Increased attention to spatial context increases both place field stability and spatial memory. *Neuron* 42, 283–295. [https://doi.org/10.1016/S0896-6273\(04\)00192-8](https://doi.org/10.1016/S0896-6273(04)00192-8).
 84. Muzzio, I.A., Levita, L., Kulkarni, J., Monaco, J., Kentros, C., Stead, M., Abbott, L.F., and Kandel, E.R. (2009). Attention enhances the retrieval and stability of visuospatial and olfactory representations in the dorsal hippocampus. *PLoS Biol.* 7, e1000140. <https://doi.org/10.1371/JOURNAL.PBIO.1000140>.
 85. Liu, X., Ramirez, S., Redondo, R.L., and Tonegawa, S. (2014). Identification and Manipulation of Memory Engram Cells. *Cold Spring Harb. Symp. Quant. Biol.* 79, 59–65. <https://doi.org/10.1101/SQB.2014.79.024901>.
 86. Tanaka, K.Z., He, H., Tomar, A., Niisato, K., Huang, A.J.Y., and McHugh, T.J. (2018). The hippocampal engram maps experience but not place. *Science* 361, 392–397. <https://doi.org/10.1126/SCIENCE.AAT5397>.
 87. Schoenenberger, P., O'Neill, J., and Csicsvari, J. (2016). Activity-dependent plasticity of hippocampal place maps. *Nat. Commun.* 7, 11824. <https://doi.org/10.1038/NCOMMS11824>.
 88. Larkin, M.C., Lykken, C., Tye, L.D., Wickelgren, J.G., and Frank, L.M. (2014). Hippocampal output area CA1 broadcasts a generalized novelty signal during an object-place recognition task. *Hippocampus* 24, 773–783. <https://doi.org/10.1002/HIPO.22268>.
 89. Brodt, S., Inostroza, M., Niethard, N., and Born, J. (2023). Sleep-A brain-state serving systems memory consolidation. *Neuron* 111, 1050–1075. <https://doi.org/10.1016/J.NEURON.2023.03.005>.
 90. Niethard, N., Ngo, H.V.V., Ehrlich, I., and Born, J. (2018). Cortical circuit activity underlying sleep slow oscillations and spindles. *Proc. Natl. Acad. Sci. USA* 115, E9220–E9229. <https://doi.org/10.1073/PNAS.1805517115/DCSUPPLEMENTAL>.
 91. Goshen, I., Brodsky, M., Prakash, R., Wallace, J., Gradinaru, V., Ramakrishnan, C., and Deisseroth, K. (2011). Dynamics of retrieval strategies for remote memories. *Cell* 147, 678–689. <https://doi.org/10.1016/J.JCELL.2011.09.033>.
 92. Frankland, P.W., Bontempi, B., Talton, L.E., Kaczmarek, L., and Silva, A.J. (2004). The involvement of the anterior cingulate cortex in remote contextual fear memory. *Science* 304, 881–883. <https://doi.org/10.1126/SCIENCE.1094804>.
 93. Niethard, N., and Born, J. (2020). A Backup of Hippocampal Spatial Code outside the Hippocampus? New Light on Systems Memory Consolidation. *Neuron* 106, 204–206. <https://doi.org/10.1016/J.NEURON.2020.03.034>.
 94. Gridchyn, I., Schoenenberger, P., O'Neill, J., and Csicsvari, J. (2020). Assembly-Specific Disruption of Hippocampal Replay Leads to Selective Memory Deficit. *Neuron* 106, 291–300.e6. <https://doi.org/10.1016/J.NEURON.2020.01.021>.
 95. Tonomi, G., and Cirelli, C. (2020). Sleep and synaptic down-selection. *Eur. J. Neurosci.* 51, 413–421. <https://doi.org/10.1111/EJN.14335>.
 96. Carr, M.F., Jadhav, S.P., and Frank, L.M. (2011). Hippocampal replay in the awake state: a potential substrate for memory consolidation and retrieval. *Nat. Neurosci.* 14, 147–153. <https://doi.org/10.1038/NN.2732>.
 97. McClelland, J.L., McNaughton, B.L., and O'Reilly, R.C. (1995). Why there are complementary learning systems in the hippocampus and neocortex: insights from the successes and failures of connectionist models of learning and memory. *Psychol. Rev.* 102, 419–457. <https://doi.org/10.1037/0033-295X.102.3.419>.
 98. Sejnowski, T.J., and Destexhe, A. (2000). Why do we sleep? *Brain Res.* 886, 208–223. [https://doi.org/10.1016/S0006-8993\(00\)03007-9](https://doi.org/10.1016/S0006-8993(00)03007-9).
 99. Lubenov, E.V., and Siapas, A.G. (2008). Decoupling through synchrony in neuronal circuits with propagation delays. *Neuron* 58,

- 118–131. <https://doi.org/10.1016/J.NEURON.2008.01.036>.
100. Miyamoto, D., Marshall, W., TONONI, G., and Cirelli, C. (2021). Net decrease in spine-surface GluA1-containing AMPA receptors after post-learning sleep in the adult mouse cortex. *Nat. Commun.* 12, 2881. <https://doi.org/10.1038/S41467-021-23156-2>.
101. van Twyver, H., Webb, W.B., Dube, M., and Zackheim, M. (1973). Effects of environmental and strain differences on EEG and behavioral measurement of sleep. *Behav. Biol.* 9, 105–110. [https://doi.org/10.1016/S0091-6773\(73\)80173-7](https://doi.org/10.1016/S0091-6773(73)80173-7).
102. Pack, A.I., Galante, R.J., Maislin, G., Cater, J., Metaxas, D., Lu, S., Zhang, L., Von Smith, R., Kay, T., Lian, J., et al. (2007). Novel method for high-throughput phenotyping of sleep in mice. *Physiol. Genomics* 28, 232–238. <https://doi.org/10.1152/PHYSIOLGENOMICS.00139.2006/ASSET/IMAGES/LARGE/ZH70150629990005.JPEG>.
103. Høydal, Ø.A., Skytøen, E.R., Andersson, S.O., Moser, M.B., and Moser, E.I. (2019). Object-vector coding in the medial entorhinal cortex. *Nature* 568, 400–404. <https://doi.org/10.1038/s41586-019-1077-7>.
104. Abeles, M., and Gerstein, G.L. (1988). Detecting spatiotemporal firing patterns among simultaneously recorded single neurons. *J. Neurophysiol.* 60, 909–924. <https://doi.org/10.1152/jn.1988.60.3.909>.

STAR★METHODS

KEY RESOURCES TABLE

REAGENT or RESOURCE	SOURCE	IDENTIFIER
Chemicals, peptides, and recombinant proteins		
paraformaldehyde	https://www.sigmaaldrich.com/	30525-89-4
isoflurane	https://www.baxter.com/	FDG9623
enrofloxacin	https://www.veterquimica.cl/	409461–409462
ketoprofen	https://www.dragpharma.cl/	naxpet
xylol	https://www.winklerltda.cl/	1330-20-7
ethylic alcohol 95%	https://www.winklerltda.cl/	2-00-427
cresyl violet acetate	https://www.sigmaaldrich.com/	10510-54-0
Experimental models: Organisms/strains		
Rat, Long-Evans	https://www.criver.com/	CrI:LE
Software and algorithms		
idTracker	http://www.idtracker.es/	N/A
MATLAB	https://www.mathworks.com/	N/A
Graphpad Prism	https://www.graphpad.com/	N/A
Other		
Epifluorescent microscope	https://www.nikon.com/	H550L
Vibratome	https://www.wpiinc.com/	NVSLM1
Stereotaxic frame	https://stoeltingco.com/	51600
Electrodes	https://calfinewire.com/	CFW2024697
Multichannel recording Amplifier	https://www.amplipex.com/	KJE-1001
Electrode interface board	https://neuralynx.com/	EIB-36
Headstages	https://intantech.com/	C3314 RHD 32-ch

RESOURCE AVAILABILITY

Lead contact

Further information and requests for resources should be directed to and will be fulfilled by the lead contact, Pablo Fuentealba (pjfuentealba@gmail.com).

Materials availability

This study did not generate new unique reagents.

Data and code availability

All data generated in this study are available upon reasonable request to the [lead contact](#). All original code generated in this study are available upon reasonable request to the [lead contact](#). Any additional information required to reanalyze the data reported in this paper is available from the [lead contact](#) upon reasonable request.

EXPERIMENTAL MODEL AND STUDY PARTICIPANT DETAILS

Adult male Long Evans rats ($n = 18$) were obtained from the Animal House Facility of the Pontificia Universidad Católica de Chile (CIBEM, <https://cibem.bio.puc.cl/>). Reporting of the age or developmental stage of subjects is also required. Animals were kept in a room with a controlled temperature ($22 \pm 2^\circ\text{C}$), in constant light/dark cycles (12:12h, 8 p.m. lights off), with water and food delivered *ad libitum*. Efforts were made to minimize the number of animals used and their suffering. Tests were conducted between 8.00 a.m. and 2.00 p.m. and all experimental procedures related to animal experimentation were approved by the Institutional Animal Ethics Committee of the Pontificia Universidad Católica de Chile (protocol code: CEBA 180703002).

METHODS DETAILS

Behavioral apparatus

The spatial memory task was performed in one of two arenas, a squared (65 × 65 cm and 35 cm height) enclosure and a circular (65 cm diameter and 35 cm height) enclosure, made of PVC. The maze was cleaned with 50% ethanol before and after each test trial. For the rest phase, the retention box was a circular plastic bucket (30 cm in diameter) where the animal could freely move. The bucket was covered with a cotton towel mounted on top, Light was provided from the top of the recording room. Noise inside the experimental room was relatively constant throughout the day (60 dB) and, in no case, exceeded 80 dB. The experimental room had 2D and 3D visual cues arranged outside the maze, yet visible to the experimental animals from the maze. The objects used for the task were glass bottles filled with corn shavings. Objects were 20–25 cm in height and were cleaned with 50% ethanol before and after each trial. Finally, the recording area was enclosed by walls and a curtain that allowed isolation of the area from the rest of the room.

Habituation

Two weeks before surgery, animal handling was performed for 10 min daily for 5 consecutive days. Then, animals were habituated to the experimental arenas and retention box. For the arenas, habituation was performed in the absence of objects. Animals were individually placed inside the arena facing the wall (alternating the entrance wall) and allowed to explore for 10 min for 3 consecutive days. For the retention box, animals spend 3 h for 3 consecutive days.

Object-place recognition (OPR) task

The behavioral task was performed once per day during the first 6 h of the light phase (8 a.m. - 2 p.m. hrs.), when the probability of NREM is larger. Two identical objects were placed 15 cm from the wall of the arena for the sample phase. The position of the objects in relation to the external cues and the rat's initial position were randomized in every phase. For the initial sample phase, animals were placed in the arena and allowed to explore for 10 min. After that, the rat was placed in the retention box for 90 min and allowed to freely sleep. Finally, for the test phase, one of the objects was displaced to the opposite quadrant in the arena. The animal was placed in the center of the arena and allowed to explore. Animal movements were video recorded for all sessions and trajectories were extracted with idTracker (<http://www.idtracker.es>). Every rat performed the OPR task once per day, alternating the arenas every day (i.e., square and circular). Thus, each rat performed a minimum of 2 sessions. Surgically implanted rats ($n = 4$) contributed with a total of 16 sessions (GV11, 2 sessions; GV12, 2 sessions; GV15, 6 sessions; and GV16, 6 sessions), whereas non-implanted rats ($n = 8$) performed a total of 22 sessions (2–3 sessions each). Moreover, pairs of objects used for the OPR task were identical in each session, but each pair was used only once for every animal. That is, animals were exposed to every pair of objects only once.

Task scoring and discrimination index

Scoring was performed by quantifying the exploration time of each object using custom-developed software in MATLAB. Behavior was considered as exploration when the rat sniffed directly at the object from maximum 2 cm. The exploration index was calculated using the exploration time of each object according to the equation.

$$\text{Exploration index} = \frac{\text{Displaced object} - \text{NonDisplaced object}}{\text{Displaced object} + \text{NonDisplaced object}}$$

Positive values of the exploration index indicate preference to explore the displaced object (novelty condition) and suggest spatial memory formation, whereas negative values indicate preference to explore the non-displaced object (familiar condition).

Stereotaxic surgery for electrode implantation

Rats were anesthetized with isoflurane (4% induction, 1.5–2% maintenance) and placed on a stereotaxic frame. Intrarectal temperature was maintained at 36–37° throughout the procedure (3–6 h) using a homeothermic blanket. The skin was incised to expose the skull, and a craniotomy (~1 mm in diameter) was made with a dental drill above the distal portion of CA1 subregion of the dorsal hippocampus in the right hemisphere (AP -3.6 mm and ML -2.2 mm from bregma). The dura was gently removed to expose the cerebral cortex in this phase. To prevent desiccation, neural tissue was lubricated with a drop of mineral oil. Eight nickel-chrome tetrodes were previously mounted in a Harlan-8 hyperdrive (Neuralynx), and each tetrode strand was connected to an EIB-36 PCB card with capacity for 32 channels. The stainless-steel wires connected two grounds to stainless steel screws that were later placed in the animal skull. One day before surgery, the impedance of each tetrode was lowered to 0.5 MOhm by coating each tip electrostatically with colloidal gold. Tetrodes were exposed 1 mm out of the metal tip of the hyperdrive and inserted in the brain with a stereotaxic guide according to the calculated coordinates; after which, craniotomy was sealed with a silicone elastomer. Two screws were placed in the occipital bone and connected as short-circuit grounds; one screw was placed in the frontal bone and one in the parietal bone of each hemisphere to serve as mechanical support. Finally, the entire surface was sealed with dental acrylic cement. The animal was hydrated with subcutaneous saline solution (NaCl 0.9%) every hour during the surgery. After surgery, rats received a daily dose of enrofloxacin (10 mg/kg, Centrovet) for five days and supplementary analgesia with ketoprofen (5 mg/kg, Centrovet) for three days. Animals had at least a week of recovery before behavioral testing.

Electrophysiological recordings

We recorded local field potentials and multiunit activity from the dorsal CA1 in a group of animals stereotaxically implanted with tetrode arrays in the dorsal CA1 stratum pyramidale (Figure S11). We recorded a total of 16 sleep sessions with their respective behavioral tasks from 4 rats. After recovery from surgery, tetrodes were lowered manually by no more than 100 μm per day. During this procedure, the EIB-36 was connected to the amplifier (Amplipex, KJE-1001) through a 32-channel headstage (HS3-Amplipex), and the electrical was checked. Recordings began when the characteristic signal of the pyramidal layer of the hippocampal CA1 sub-region was observed, such as large-amplitude theta waves, ripples, and an abrupt increase in the density of units. One tetrode was used as reference, and continuous recordings were performed and digitized at 20,000 samples per second. Each session was also video recorded synchronized with the amplifier clock. After recordings, the obtained DAT files were transformed to MATLAB format for further analyses using the LAN toolbox (<http://lantoolbox.wikispaces.com/>). Recordings were continuously performed during the entire OPR task, that is, sample, rest and test phases were all included in one single file.

Histology and recording site identification

After recordings, animals were anesthetized with isoflurane, electrolytically lesioned in each tetrode (10 μA positive current for 10 s was applied to every pair of channels), and allowed to recover for 48 h. After that, rats were terminally anesthetized and intracardially perfused with a saline solution followed by a 20 min fixation with 4% paraformaldehyde. Brains were extracted and postfixed in paraformaldehyde overnight before being transferred to PBS-azide and sectioned coronally (60–80 μm slice thickness). Sections were further stained for Nissl substance. Locations of recording sites were performed under a light transmission microscope.

Sleep scoring

Sleep scoring of non-implanted animals was performed visually according to the movement of the animals. We defined sleep as continuous periods of immobility laying down of at least 10 s. This criterion was based on similar studies that visually scored sleep.^{38,39} This technique has been previously employed in both our own and others' research in rodents. This method has demonstrated a high level of agreement (reaching 92%) when compared to the EEG/EMG-based scoring method.^{42,101,102} For implanted animals, in addition to immobility, sleep scoring was performed using an electrode positioned in the hippocampal dorsal CA1 pyramidal layer.⁴¹ The LFP signal from this electrode was downsampled to 1000 Hz, and time-frequency decomposition was performed with Fourier analysis using the LAN toolbox to obtain the signal's power spectral density. The signal was analyzed for subsequent 10-s windows, where the raw LFP signal, the power spectrum, and the video recording were used to determine the stage of the sleep-wake cycle. One of three different stages was assigned to each window depending on the following criteria: if the power spectrum had a peak in slow wave activity (0.5–4 Hz) and the animal was immobile, the window was identified as NREM; if the power spectrum presented a peak in theta oscillations (4–10 Hz) and the animal was immobile, the window was identified as REM sleep; finally, if the animal was actively moving, the window was identified as awake. To assign a window into any of these categories, the criteria had to be fulfilled in at least 50% of the window. Exceptionally, a window was scored as undetermined if the previously described criteria were not met. This analysis was performed with a MATLAB (MathWorks, Natick, MA) script.

Sleep oscillations

Theta oscillations were detected by calculating the continuous ratio between the envelope of theta (4–8 Hz) and delta waves (1–4 Hz) frequency bands filtered from the hippocampus LFP and computed by the Hilbert transform. A ratio of 1.4 standard deviation (SD) or higher during at least 2 s defined epochs of theta oscillations.

For the detection of ripples, the LFP signal was downsampled to 1 kHz and band-pass filtered (100–250 Hz) using a zero-phase shift non-causal finite impulse filter with 0.5 Hz roll-off. Next, the signal was rectified, and low-pass filtered at 20 Hz with a fourth-order Butterworth filter. This procedure yields a smooth envelope of the filtered signal, then a Z score normalized using the whole signal's mean and SD. Epochs during which the normalized signal exceeded a 3 SD threshold and 50 ms of duration were considered ripples. The first point before the threshold that reached 1 SD was considered the ripple onset, and the first point after the threshold to reach 1 SD was considered the ripple end. The difference between onset and end of ripples was used to estimate the ripple duration. We introduced a 50 ms-refractory window to prevent double detections. To precisely determine the mean frequency, amplitude, and duration of each ripple, a spectral analysis using Morlet complex wavelets of seven cycles was performed. The protocol was adapted from a previously described method,²² and the LAN toolbox (<http://lantoolbox.wikispaces.com/>) was used for the implementation.

Spindles were detected in the downsampled hippocampal LFP signal (1 kHz), by calculating the maximum normalized wavelet power from the filtered signal (11–17 Hz). This signal was then Z score normalized, using the whole signal's mean and SD. Epochs during which the normalized signal exceeded a 1.4 SD threshold and 350 ms of duration were considered spindles. Spindles considered for analysis were exclusively detected during NREM epochs.

Slow wave activity was detected by calculating the envelope of the slow oscillations (0.5–4 Hz) filtered from the hippocampus LFP and computed by the Hilbert transform. Slow wave activity was Z-scored during all sleep periods and epochs with amplitude 1.4 SD or higher, and at least 2 s were defined as slow wave activity.

Spike sorting

To investigate the spike timing of individual neurons during distinct brain states, we performed spike sorting of multiunit activity from the dorsal hippocampus. Neuronal spikes were extracted from hippocampal recordings using the semiautomatic clustering program Klustakwik (<https://github.com/kwikteam/klustakwik2/>). This method was applied over the 32 recording channels (8 tetrodes), after the signals were filtered between 300-5,000 Hz. Spike clusters were considered single units if less than 1% of their spikes had an interspike interval below 1 ms, and their auto-correlograms had a 2 ms-refractory period. Single units were stable during recording sessions and their amplitude did not vary significantly during sleep (Figure S12).

Place cells

Place cells were identified during arena exploration in the sample and test phases of the task. Only data from epochs in which the animal ran faster than 5 cm/s were considered to identify place cells between hippocampal units. Each arena was divided into 5x5-cm bins, where the time the animal spent in each bin was sorted to obtain an occupancy map. The animal's position on the arena was determined by detecting a LED placed on the animal's headstage recorded at 30 fps. Spikes from each unit were sorted in map bins to obtain the firing map. Next, the firing rate was calculated using time and spikes in each bin to compute a firing rate map. A Gaussian kernel (SD = 7 cm) was applied to firing rate maps to obtain smoothed maps used to compute spatial map parameters.

The mean firing rate on the arena was calculated from all bins where the animal spent at least 100 ms. The peak firing rate corresponded to the highest firing rate detected in the visited bins. Sparsity, which represents the proportion of the arena where a unit fires, was obtained by using the equation:

$$\text{sparsity} = \frac{\pi * \lambda_i^2}{\lambda^2}$$

Where π is the probability of occupancy of a specific bin, λ_i is the firing rate in that bin, and λ is the mean firing rate. Finally, place fields were defined as the contiguous area starting from location of the unit's peak firing rate, until it reached 2 SD of the average firing rate in the firing rate map (adapted from.¹⁰³ Only contours that bounded an area of at least 6 bins (150 cm²) were identified as place fields. After visual inspection of the putative place fields in the smoothed maps, that threshold was established to avoid false positives resulting from random firing in scarcely visited regions.

We fitted a sigmoid function to the distribution of all recorded units during the sample phase. The mean firing rate (log scale) versus overall sparsity of all units was plotted and fitted to a sigmoid curve using the MATLAB curve fitting toolbox from which the critical values were obtained. The relation resulting from this analysis was:

$$\text{overall sparsity} = \frac{1}{1 + \exp^{-0.72 * \log \text{ firing rate}}}$$

We obtained the lower and upper inflection points from this fit, which delimit the linear zone of sigmoid fit, depicting the zone where place cells are located. This allowed to us discard from place analysis units with low firing rates (<0.18 Hz) and high sparsity (>0.78) in our experiments. Shifting these thresholds produced similar results to those reported in the current study.

Units with firing rates larger than 0.18 Hz (lower critical point in the sigmoid fit), sparsity lower than 0.78 (upper critical point in the sigmoid fit), and showing of at least 1 place field, were classified as place cells. For sparsity, shufflings of 1,000 iterations were carried out for the spike timestamps from each single unit, maintaining the animal trajectory unchanged. Sparsity values for each iteration were used to compute the Z score value, discarding units that did not reach 1.5 SD. This threshold was defined after visual inspection of the putative place cells in the smoothed map.

Units that did not meet these criteria were classified as non-spatial cells. This classification was performed in both sample and test phases of the task.

Peri-event cross-correlograms

Hippocampal ripples and neuronal spikes were cross-correlated by applying the 'sliding-sweeps' algorithm.¹⁰⁴ A time window of ± 1 s was defined with the 0-point assigned to the onset of a ripple. The timestamps of spikes within the time window were considered as a template and were represented by a vector of spikes relative to $t = 0$ s, with a time bin of 25 ms and normalized to the total number of spikes. Thus, the central bin of the vector contained the ratio between the number of thalamic spikes elicited between ± 12.5 ms and the total number of spikes within the template. Next, the window was shifted to successive events (i.e., spikes or oscillatory events) throughout the recording session, and an array of recurrences of templates was obtained.

Population vector

In each task trial, the spatial maps associated to each unit were assembled in a 3D matrix, where the z axis corresponded to the different units recorded in the trial. Using this matrix, a population vector was generated with the firing rate values from all units in every spatial bin.⁵⁶ Such a matrix was constructed for both the sample and test phases. The Spearman correlation between both sample and test population vectors was computed, thus obtaining a correlation coefficient (r) for each session.

QUANTIFICATION AND STATISTICAL ANALYSIS

Statistical analysis

Normally distributed parameters were analyzed with parametric tests (one-way ANOVA followed by Bonferroni corrected post-hoc t-test). Comparisons between non-normally distributed parameters were analyzed with non-parametric analysis (Kruskal-Wallis test followed by Tukey's multiple comparison *post-hoc* test). Linear correlations between parameters were analyzed using Spearman correlation coefficients. Comparison between peri-event time histograms were analyzed with Wilcoxon test. Causal mediation analysis was calculated with the R-package 'mediation', which calculates an average causal mediation effect (ACME) and an average direct effect (ADE) between the correlated variables. Statistical analysis was performed with Graphpad Prism software or with MATLAB (The Mathworks Inc.). Significant differences were accepted at $p < 0.05$.